Heliyon 9 (2023) e21413

Contents lists available at ScienceDirect

Heliyon

journal homepage: www.cell.com/heliyon

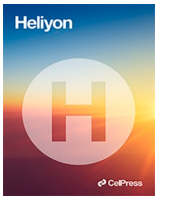

Bio-sorptive remediation of crude oil polluted sea water using plantain (*Musa parasidiaca*) leaves as bio-based sorbent: Parametric optimization by Taguchi technique, equilibrium isotherm and kinetic modelling studies

Blessing E. Eboibi [a,c], Michael C. Ogbue [b], Esther C. Udochukwu [c], Judith E. Umukoro [a], Laura O. Okan [a], Samuel E. Agarry [c,d,**], Oluwafunmilayo A. Aworanti [d,***], Oyetola Ogunkunle [e,*], Opeyeolu T. Laseinde [e]

[a] *Biochemical and Bioenvironmental Engineering Laboratory, Department of Chemical Engineering, Delta State University, Abraka, P. M. B. 22, Oleh Campus, Nigeria*
[b] *Department of Petroleum Engineering, Delta State University, Abraka, P. M. B. 22, Oleh Campus, Nigeria*
[c] *Department of Chemical Engineering, Federal University, Otuoke, Nigeria*
[d] *Biochemical and Bioenvironmental Engineering Research Group, Department of Chemical Engineering, Ladoke Akintola University of Technology, P. M. B. 4000, Ogbomoso, Nigeria*
[e] *Department of Mechanical and Industrial Engineering Technology, University of Johannesburg, South Africa*

ARTICLE INFO

Keywords:
Biosorptive remediation
Biosorption kinetics
Crude oil
Plantain leaves
Optimization
Taguchi design

ABSTRACT

This study investigated the potential of employing plantain leaves as a natural bio-based sorbent for crude oil spill polluted seawater remediation. Type $L_9(3^4)$ Taguchi orthogonal array technique was used to evaluate the effect of four independent bio-sorption factors at three different levels (crude oil initial concentration (X_1 7.8, 11.5 and 15.6 g/L), seawater-crude oil temperature (X_2 25, 35 and 45 °C), bio-sorbent dosage (X_3 1, 2 and 3 g) and bio-sorbent particle size (X_4 1.18, 2.36 and 4.72 mm) on two response indices (bio-sorption efficiency (%) and bio-sorption capacity (g/g)). Taguchi optimization technique, numerical-desirability index function optimization technique and a proposed optimization method were utilized to determine the optimum bio-sorption factors needed for the optimum bio-sorption efficiency and bio-sorption capacity. The results demonstrated that the crude oil bio-sorption efficiency of the plantain leaves was significantly influenced by X_1, X_3 and X_4 and the bio-sorption capacity was mainly influenced by X_1 and X_3. The optimum bio-sorption efficiency and the optimum bio-sorption capacity were 99.05 % and 12.82 g/g, respectively, obtained at optimum combination of factors and levels of X_{11} (7.8 g/L), X_{33} (3 g) and X_{41} (1.18 mm) for bio-sorption efficiency and X_{13} (15.6 g/L) X_{31} (1 g) for bio-sorption capacity. The Freundlich and Dubinin-Rudeshkevich isotherm models best explain the equilibrium bio-sorption data, while the pseudo-second order kinetic model best describes the bio-sorption kinetics. The bio-sorptive remediation mechanism followed dual mechanism of physical and chemical bio-sorption and the mass transfer controlled by film diffusion. The maximum bio-sorption capacity (K_f) was 14.0 gg^{-1}.

* Corresponding author.
** Corresponding author. Department of Chemical Engineering, Federal University, Otuoke, Nigeria.
*** Corresponding author.
E-mail addresses: seagarry@lautech.edu.ng (S.E. Agarry), oaaworanti@lautech.edu.ng (O.A. Aworanti), oogunkunle@uj.ac.za (O. Ogunkunle).

https://doi.org/10.1016/j.heliyon.2023.e21413
Received 18 July 2023; Received in revised form 10 October 2023; Accepted 20 October 2023
Available online 3 November 2023

1. Introduction

Water pollution by crude oil due to spillage during offshore production and transportation has been a major challenge that is been faced by oil producing countries like Nigeria, which requires rapid remedial response. This is because crude oil being a mixture of several different hydrocarbons including alkanes and polycyclic aromatic hydrocarbons (PAHs), its pollution in surface and subsurface sources leads to serious significant long term hazardous and toxicological effect on human life and the ecosystem as well as results in economic losses [1]. Therefore, there is the need for its removal and clean-up as quick as possible to prevent the deleterious effect.

The removal or clean-up can be performed through applying physical/mechanical, chemical and biological methodologies [2]. The physical/mechanical methods entails using booms, skimmers and sorbents [3,4] as well as burning [5] and the chemical method involves the usage of chemical dispersants [6] while the biological method entails the usage of microorganisms (bioremediation) [7]. Nevertheless, the removal or clean-up of crude oil spillage in water employing the usage of sorbents have in recent years received increasing attention due to their simple applicability and cost-effectiveness [1,3].

Sorbents are materials that are either inorganic (such as glass) [5], organic (e.g. agricultural biomass) or synthetic (like polyurethane) [8], which are porous and can bind to varying types of inorganic chemicals (e.g. heavy metals) and organic chemicals by surface adsorption and/or absorption as the case may be [1]. The sorbents utilized for oil spillage remediation should be hydrophilic or oleophilic (oil-loving) and hydrophobic (water-hating) and should as well possess other characteristics which includes high buoyancy, biodegradable, high uptake of oil or sorption capacity, low-cost and reusability [3,9]. Varying synthetic sorbent types such as magnetic Fe_3O_4/polystyrene nanoparticles [10], polyurethane sponge [11] and graphene-wrapped sponge [12] have been examined for their potential crude oil removal or clean-up and were detected or observed to have different efficiencies. But due to these synthetic sorbents being non-renewable and non-biodegradable, which can easily cause environmental nuisance or pollution, there is an increasing interest in developing biodegradable natural materials as bio-based sorbents [2]. Natural bio-based sorbents such as agricultural waste materials or biomass have shown good performance in oil removal or clean-up of oil spill [2]. Some of the natural bio-based sorbents that have been employed for clean-up of oil includes, rice husk [13], wheat husk [14], date palm fibre [3], avocado peel [15], cocoa pod [16], peat-derived biochar [1], corncobs [17], plantain peels [18], coconut husk [19], mango seed shell [20], plantain peel-derived activated carbon [21] and empty bunch of oil palm's fruit [2]. However, the need to still develop other natural agricultural-based biomass that are readily and abundantly available as bio-based sorbents for oil spill remediation which are of low-cost with high sorption capacity is further required. Although fewew agricultural plant leaves like pineapple leaves [22], *Ricinus communis* leaves [23], Neem leaves [24], *Cissus populnea* leaves [25], *Lawsonia* leaves [26], and spent tea leaves [27] have been employed for oil-water biosorptive remediation, however, to the best of our knowledge, information on the potential utilization of plantain leaves as a bio-based sorbent for oil spill-water remediation is still very scarce or limited. Plantain leaves are readily and abundantly available in the South-West and Niger-Delta regions of Nigeria. Thus, concerted attempts have been made by the authors to leverage on the plantain leaves' availability and abundance for usage as natural bio-based sorbent for remediating or cleaning up oil spill.

In addition, conventional experimental optimization method often named as one variable-at-a-time (OVAT) is usually executed by varying one variable level at a time over a desired range and monitoring its effect or influence on the experimental response (output) while other test variables' levels are kept constant. This is repeated for every other test variable and thus results to large number of experiments which in the overall makes the process to be cumbersome, costly, labour and time consuming [28]. Thus, employing multivariate statistical optimization techniques which entails experimental design utilization, helps to a large extent to overcome these OVAT challenges or problems [4,28]. Among the most commonly and important multivariate statistical optimization techniques utilized is the Taguchi orthogonal array technique (TOAT). The TOAT is a powerful and unique technique of optimization that allows optimization with minimal experimental numbers [29]. It employs the usage of orthogonal arrays that distributes the factors or variables in a well-balanced manner where the effect of each factor on the response mean and variation can independently be investigated and estimated [20,30,31]. The experimental response is converted into a signal-to-noise ratio (S/N) which allows for the factors optimum values to be easily determined [31]. TOAT has been applied to optimize pollutant bio-sorption such as inorganic chemicals or heavy metals [28,32], organic chemicals [33], dyes [34] and petroleum hydrocarbons' bioremediation in water [35]. However, using TOAT for the optimization study of petroleum hydrocarbons' polluted water bio-sorptive remediation is still very scarce.

Thus, the major goal of this work was to investigate plantain leaves' potential or feasibility as natural bio-based sorbents for crude oil polluted seawater remediation. The specific objectives were to: (i) investigate the major effects of crude oil initial concentration, bio-sorbent particle size, bio-sorbent dosage and crude oil-seawater temperature on the crude oil bio-sorption efficiency and bio-sorption capacity of plantain leaves as well as determining the bio-sorption optimum conditions required for maximum bio-sorption efficiency and maximum bio-sorption capacity using the TOAT; and (ii) propose an optimization model and to model the equilibrium bio-sorption and the crude oil-water pollution bio-sorptive remediation kinetics. Fourier transform infra-red spectroscopy (FTIR) and scanning electron microscopy (SEM) was conducted on the plantain leaves to assess their surface characteristics and elucidate the bio-sorption mechanism.

2. Materials and methods

Nigerian crude oil was employed for the research work. The crude oil properties were as follows: density, 0.78 g/cm^3. API, 35.91° and viscosity, 4.75 cSt. Utilized for the remediation studies was a simulated seawater. Analytical grade reagents and chemicals (Sigma-

Aldrich, Germany) were utilized. Raw plantain leaves' samples adopted for the bio-sorptive remediation were gotten from a small plantain plantation located at Iyede town in Delta State of Nigeria.

2.1. Simulated seawater preparation

The seawater that was simulated was made by adding into distilled water (1 L), 20 g of sodium chloride (NaCl) salt [36]. The resultant solution was thoroughly agitated with a stirring rod.

2.2. Preparation and characterization of bio-sorbent

The plantain leaves were washed, firstly with tap water and later with distilled water, after which they were dried in the sun for seven days and thereafter dried in the oven at 105 °C for 6 h. The dried leaves were then crushed making use of laboratory mortar and pestle and finally grounded into small particles using a grinding machine. The grounded plantain leaves' particles were sieved to obtain different particle sizes of 1.18 mm, 2.36 mm and 4.72 mm, respectively. The grounded plantain leaves of different particles were packaged in different plastic bottles prior to utilization.

The specific surface area and pore size distribution of the plantain leaves' biosorbent were determined using the Brunauer-Emmett-Teller-Nitrogen (BET-N_2) surface area analyzer (Micromeritics Tristar II 3000), which consisted of three analysis ports that were operated simultaneously. A canister of liquid nitrogen was used for the adsorption and desorption processes.

The porosity of the plantain leaves' particles was determined employing the modified liquid saturation method [37]. Using this method, the weight of plantain leaves' particles was taken and recorded (P_1). Slightly mineralized water (mineralization of 5 g/L sodium chloride in deionized water) and kerosene were utilized as saturation fluids. This saturation fluid was allowed to saturate the samples under vacuum pressure for about 10–15 s. The particles were thoroughly mixed in the saturating fluid to remove air from the intergranular space. Thereafter, the saturated particles were weighed and recorded (P_2). After this, the saturated plantain leaves' particles were further saturated in a high-pressure vessel for 2 days at a pressure of 20 MPa, after which the weight was recorded (P_3). The porosity (K_P) of the plantain leaves' particles was calculated using Equation 1a - c [37]:

$$\%K_P = \frac{\rho_{particle} - \rho_{bulk}}{\rho_{particle}} \times 100 \tag{1a}$$

$$\rho_{bulk} = \frac{P_1}{P_1 - P_2}\rho_f \tag{1b}$$

$$\rho_{particle} = \frac{P_1}{P_1 - P_3}\rho_f \tag{1c}$$

where K_P – open porosity, %; ρ_{bulk} – bulk density, g/cm^3; $\rho_{particle}$ – particle density, g/cm^3; P_1 – mass of dry sample in air, g; P_2 – mass of dry sample immersed in saturating fluids, g; P_3 – mass of saturated sample immersed in saturating fluid, g; ρ_f – density of saturating fluid, g/cm^3.

In determining the functional groups that characterize the plantain leaves' bio-sorbent, Fourier transform-infrared (FT-IR) spectrophotometer (Spectrum 65, PerkinElmer model) which involves the usage of potassium bromide as an agent was employed. At a frequency range of 400–4000 cm^{-11}, the FT-IR spectra was recorded. The morphology of the bio-sorbent surface before crude oil biosorption and after crude oil bio-sorption was determined using the scanning-electron- microscopy (SEM, Joel JSM 6360LA, Japan). In using this SEM, the bio-sorbent samples were put on aluminum stubs and then vacuum-coated with gold before they were examined by SEM. The water and oil wettability or hydrophilic and hydrophobic nature, of the biosorbent surface was determined by measuring the contact angle that exists between the biosorbent and the liquid (water or oil) using a drop shape analyzer device (Krüss Drop Shape Analysis System DSA 10 Mk2).

2.3. Determination of the degree of hydrophobicity (HD)

In determining the sorbent's HD, the Agarry et al. [4] procedure was adopted. This procedure involved adding 1 g of the bio-sorbent into 20 mL of distilled water contained in a 50 mL beaker and vigorously agitated. Into the bio-sorbent-water mixture was added 20 mL of hexane and thoroughly mixed together for 3 min and afterwards left for 5 min to give room for the two immiscible organic and aqueous phases to separate. The quantity of bio-sorbent present in the organic phase was attained from the filtration of the organic phase. The filtered bio-sorbent was oven-dried and weighed. Using Equation (2), the sorbent's HD was calculated:

$$HD(\%) = \left[\frac{W_H}{W_O}\right] \times 100 \tag{2}$$

Where, W_H and W_O are the bio-sorbent's weight in organic phase (g) and original bio-sorbent's weight (g), respectively. The plantain leaves' HD was obtained as 19.8 %.

2.4. TOAT experimental design for polluted seawater remediation

TOAT experimental design selected factors and levels are presented in Table 1.

Table 1 shows four factors and three levels utilized in the experiment. On the background of fractional factorial technique of Taguchi's optimization, the number of experimental runs, N can be determined by $N = 2w + 1$, where w is total number of factors [33]. In this case, for 4 bio-sorption factors, N = 9 thus, L9 orthogonal array for 3 selected level (Table 1) was obtained. The array reduces the $3^4 = 81$ number of experimental runs into 9 experimental runs. Therefore, the TOAT of L_9 (3^4) type (i.e., four factors with three levels each and 9 experimental runs) was utilized (Table 2).

The crude oil initial concentration (X_1), seawater-crude oil temperature (X_2), bio-sorbent dosage (X_3) and bio-sorbent particle size (X_4) were assigned to the 1st, 2nd, 3rd and 4th column of L9 array respectively (Table 2). The experiment was conducted in line with Table 2 design. Into a 50 mL beaker was added 30 mL of simulated seawater and 11.7 g of crude oil was weighed (equivalent to 10 mL) and introduced into it. A known gram (i.e., 1 g) of the bio-sorbent sample was weighed and spread over the oil-seawater polluted system and the system was left at ambient or laboratory temperature (25 °C) for 15 min to allow for remediation to take place without any form of agitation. The saturated oil-water adsorbed bio-sorbent sample was taken out at the end of 15 min with stainless steel mesh screen and then permitted to drain for 8 min. Thereafter, the saturated oil-water adsorbed bio-sorbent was weighed. The n-hexane solvent extraction method described in ASTM D1533 and ASTM D4007-81 was utilized to find out the water sorbed by the bio-sorbent sample. Batch equilibrium and kinetic studies were performed for different crude oil initial concentrations (3.9, 7.8, 11.7 and 15.6 g/L). However, the oil-water adsorbed bio-sorbent was removed at different time intervals of 3 min up till 15 min of incubation or remediation time. Triplicate experiments were performed, and their average values were employed for calculations. The adsorbed oil quantity at time, t (q_t, g/g) (i.e. bio-sorption capacity) was calculated based on Equation (3) [3]:

$$Biosorption\,Capacity\,(q_t) = \frac{Mass\,of\,Oil\,Removed\,(g)}{Mass\,of\,Biosorbent\,(g)} \tag{3}$$

The bio-sorption efficiency (i.e., oil-removal efficiency) was computed utilizing Equation (4) [3]:

$$Biosorption\,Efficiency\,(\%) = \frac{Mass\,of\,Oil\,Removed}{Initial\,Mass\,of\,Oil} \times 100 \tag{4}$$

2.5. Modelling of the optimization process by Taguchi method

In $L_9(3^4)$ type of TOAT, there are no factors' interaction. Thus, the obtained bio-sorption efficiency and bio-sorption capacity results' data were fitted to a factorial linear regression model (Equation (5)) [38] employing the Design-Expert software (version 13) to derive the statistical model equation for the prediction of the optimum output response during the crude oil polluted seawater bio-sorptive remediation.

$$Y = \beta_o + \sum_{j=1}^{n} \sum_{i=1}^{m} X_{ij} f_x(\beta) \tag{5}$$

where Y = output response; $ß_o$ = an intercept; X_{ij} = ith factor with jth level; f_x (ß) = $ß_{ij}$ which denotes the linear regression coefficients. F-test and *P*-values were chosen to determine each coefficient in the equation's significance. An optimization model proposed by Serencam et al. [38] based on Equation (5) was applied and the optimization model is provided in Equation (6):

$$Maximize\,Y : \text{Subject to the constraints:} (1)\ \sum_{i=1}^{m} X_{ij} = 1 (j = 1, 2, .., n) \tag{6}$$

$$(2)\ X_{ij} \in \{0, 1\}$$

The proposed model objective is to maximize the regression function (i.e. the output response) in Equation (6)) ascribed to the "Highest is best or Larger is better" (HB or LB-type) quality characteristics.

Table 1
Process selected factors and their levels.

Symbol	Factors	Levels		
		1	2	3
X_1	Crude Oil Initial Concentration (g/L)	7.8	11.7	15.6
X_2	Seawater-Crude Oil Temperature (°C)	25	35	45
X_3	Bio-Sorbent Dosage (g)	1	2	3
X_4	Bio-Sorbent Particle Size (mm)	1.18	2.36	4.72

Table 2
Experimental layout using an L_9 (3^4) orthogonal array.

Experimental Run	Main factors							
	X_1		X_2		X_3		X_4	
	Coded	Actual	Coded	Actual	Coded	Actual	Coded	Actual
L1	1	7.8	1	25	1	1	1	1.18
L2	1	7.8	2	35	2	2	2	2.36
L3	1	7.8	3	45	3	3	3	4.72
L4	2	11.7	1	25	2	2	3	4.72
L5	2	11.7	2	25	3	3	1	1.18
L6	2	11.7	3	45	1	1	2	2.36
L7	3	15.6	1	25	3	3	2	2.36
L8	3	15.6	2	35	1	1	3	4.72
L9	3	15.6	3	45	2	2	1	1.18

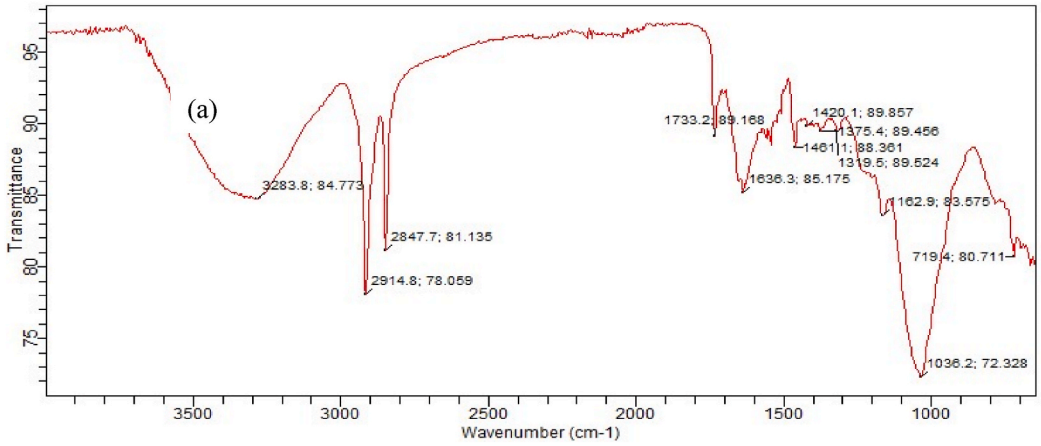

(a) Before bio-sorption

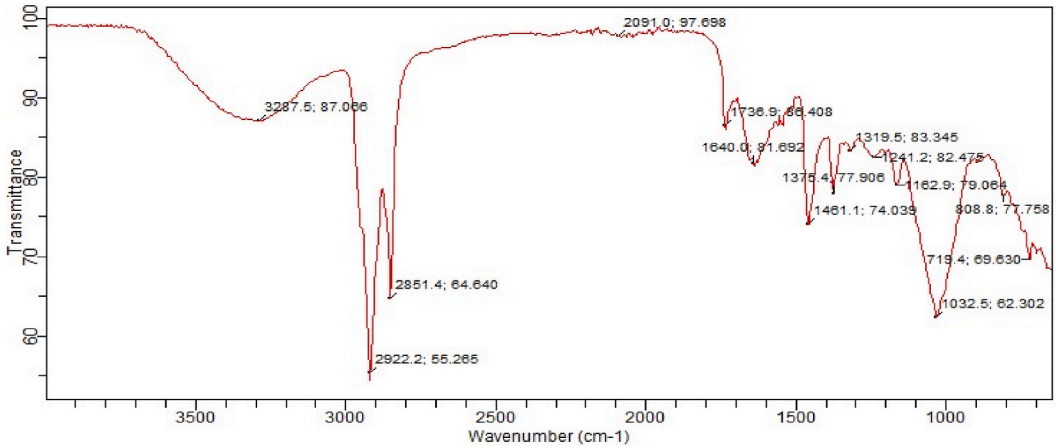

(b) After bio-sorption

Fig. 1. Plantain leaves-bio-sorbent FTIR spectra. (a) Before bio-sorption (b) After bio-sorption at crude oil initial concentration of 7.8 g/L, seawater-crude oil temperature of 30 °C, bio-sorbent dosage of 3 g and bio-sorbent particle size of 1.18 mm.

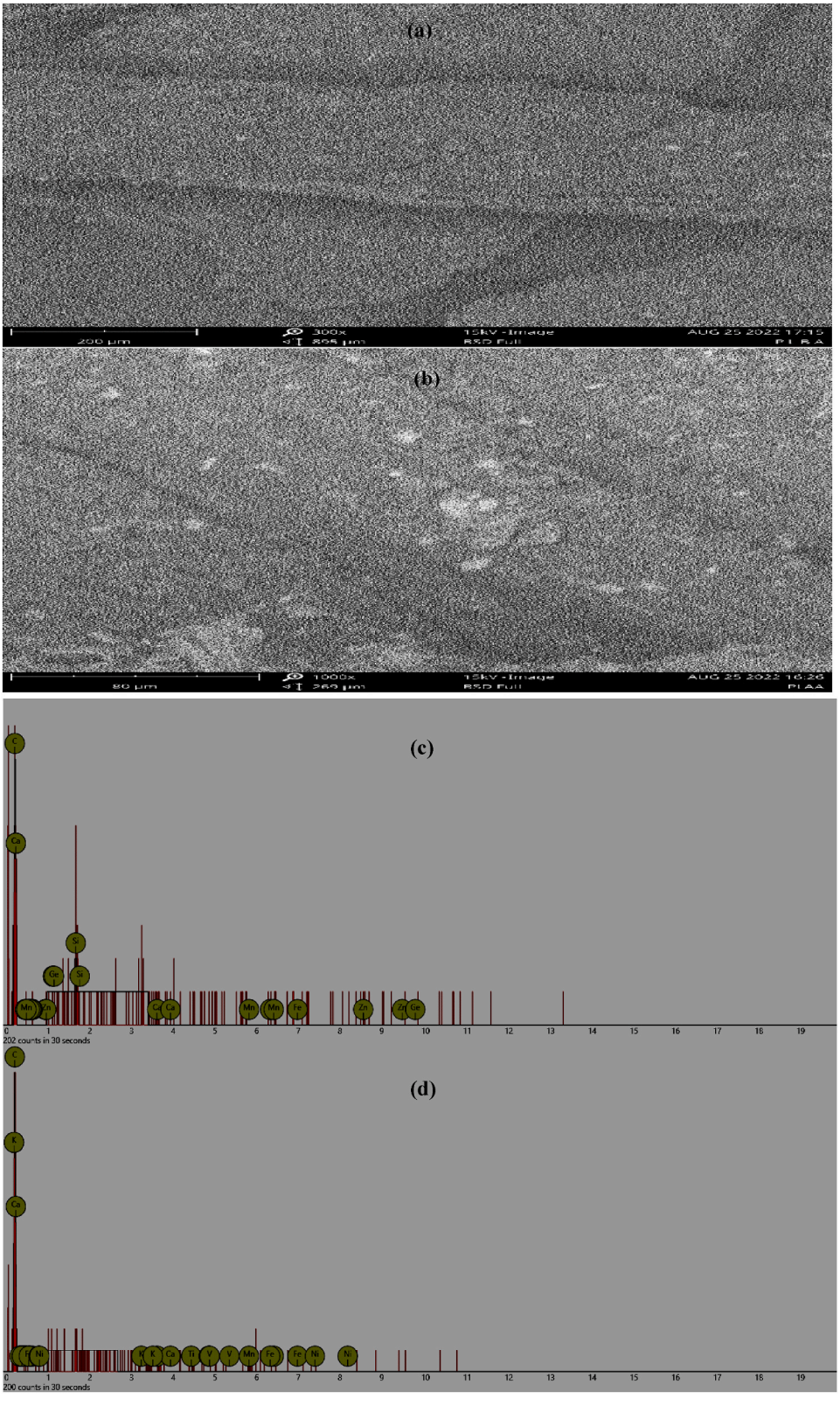

(caption on next page)

Fig. 2. (a) SEM of plantain leaves before bio-sorption (@ 200 μm magnification). (b) SEM of plantain leaves after crude oil bio-sorption at crude oil initial concentration of 7.8 g/L, seawater-crude oil temperature of 30 °C, biosorbent dosage of 3 g and biosorbent particle size of 1.18 mm (@ 200 μm magnification). (c) EDX of plantain leaves before bio-sorption. (d) EDX of plantain leaves after crude oil bio-sorption at crude oil initial concentration of 7.8 g/L, seawater-crude oil temperature of 30 °C, biosorbent dosage of 3 g and biosorbent particle size of 1.18 mm.

2.6. Experimental bio-sorptive remediation data analysis

Experimental remediation result data garnered from utilizing $L_9(3^4)$ TOAT were analyzed using the variance analysis (ANOVA) and the signal-to-noise ratio (S:NR). The signal term stands for the mean (desirable value) and the noise term represents the standard deviation (undesirable value) for the output response characteristics [31] or good:error ratio [33]. That is, S: NR represents output quality or characteristics. The S: NR ratio was employed to select the optimum level of the significant factors that maximizes this ratio. The S: NRs were computed for the bio-sorption efficiency and bio-sorption capacity, respectively. The S: NR equation presented in Equation (7) [31,33] for the criterion "HB or LB-type" quality characteristics was applied.

$$\frac{S}{N} = -\log 10\left[\frac{1}{n}\sum_{i=1}^{n}\left(\frac{1}{y}\right)^2\right] \tag{7}$$

where y is the output response and n is the number of tests' trial for a particular experimental run.

3. Results and discussion

3.1. Characterization of plantain leaves-bio-sorbent using FTIR

The FTIR carried out on the plantain leaves as bio-sorbent before crude oil bio-sorption and after crude oil bio-sorption resulted in the illustrated FTIR spectra in Fig. 1.

The plantain leaves' FTIR spectra before crude oil bio-sorption (Fig. 1(a)) revealed several absorption wavelength peaks which indicates different functional groups. Fig. 1(a) shows the occurrence of a strong broad band peak at 3287.5 cm^{-1}, which was assigned to the hydroxyl group (OH) stretching vibrations that exist in cellulose, hemicellulose and lignin of plantain leaves [2,23] and to N–H stretching vibrations [9]. The absorption band peaks that appeared in the region of 2851.4 and 2922.2 cm^{-1} were attributed to C–H asymmetric and symmetric stretching of alkane CH_2 and CH_3 [23,39–41]. Absorption band peak at 1738.9 cm^{-1} was ascribed to the carbonyl (C═O) functional group stretching of ester or amide that occurs in hemicellulose [4,16,39]. The two absorption band peaks observed at 1461.1 and 1640.0 cm^{-1} corresponded to the presence of C═C- stretching vibrations of aromatic ring [23,41,42]. The two absorption band peaks that occurred at 1319.5 and 1375.9 cm^{-1} were ascribed to C–O skeletal vibrations and OH bending [43]. The observed peaks at 1162.9 and 1241.2 cm^{-1} were assigned to C–OH bending and -C-*O*-C stretching in hemicellulose [44,45]. Also, the peak found at 1032.5 cm^{-1} was considered to be attributable to C–O, C–O–H and C–O–C stretching vibrations in cellulose and hemicellulose [9,23,29,31,46] while the two absorption bands observed at 719.4 and 808.8 cm-1 were assigned to C–Cl stretch and

Table 3
SEM-EDX results for plantain leaves before and after crude oil bio-sorption at crude oil initial concentration of 7.8 g/L, seawater-crude oil temperature of 30 °C, bio-sorbent dosage of 3 g and bio-sorbent particle size of 1.18 mm.

Before crude oil bio-sorption				
Element number	Element symbol	Element name	Atomic concentration	Weight concentration
6	C	Carbon	87.17	62.20
30	Zn	Zinc	3.69	14.34
32	Ge	Germanium	2.69	11.60
26	Fe	Iron	0.94	3.13
14	Si	Silicon	1.57	2.62
20	Ca	Calcium	0.90	2.15
8	O	Oxygen	1.87	1.77
25	Mn	Manganese	0.40	1.31
9	F	Fluorine	0.77	0.87
After crude oil bio-sorption				
Element number	Element symbol	Element name	Atomic concentration	Weight concentration
6	C	Carbon	89.28	75.18
8	O	Oxygen	5.52	6.19
25	Mn	Manganese	1.37	5.28
22	Ti	Titanium	1.18	3.96
28	Ni	Nickel	0.84	3.46
26	Fe	Iron	0.54	2.12
20	Ca	Calcium	0.72	2.02
23	V	Vanadium	0.33	1.17
19	K	Potassium	0.22	0.61

alkyne C–H bend [42]. In a similar fashion, the same kind of FTIR spectra were obtained for the plantain leaves bio-sorbent after crude oil bio-sorption (Fig. 1(b)). However, in this particular case, slightly lower absorption band peaks were observed at 3283.8 cm^{-1}, 2847.8 cm^{-1}, 2914.8 cm^{-1}, 1733.2 cm^{-1}, 1636.3 cm^{-1}, 1420.1 cm^{-1}, and slightly higher peak at 1038.2 cm^{-1} while the peak at 1241.2 cm^{-1} observed in Fig. 1(a) was not seen in Fig. 1(b). The slightly observed lower and higher band peaks along with the observed missing peak were peaks that were attributable to hydrophobic or hydrophilic functional groups, thus confirmed that the crude oil actual bio-sorption occurred at these plantain leaves' hydrophobic sites [16].

3.2. SEM-EDX characterization of bio-sorbent

Fig. 2 shows the micrographs of the SEM-EDX carried out on the plantain leaves bio-sorbent before and after crude oil bio-sorption, which depicts their surface morphologies.

It was obviously seen that the plantain leaves bio-sorbent before bio-sorption has a smooth and homogeneous surface with high porous texture (Fig. 2(a)) and contained major elements such as carbon, zinc and germanium with weight percentage amount of 62.20, 14.34 and 11.60, respectively. However, it also contained several other elements like iron, silicon, calcium, oxygen, manganese and fluorine in minor quantities (Fig. 2(c) and Table 3). However, after the crude oil bio-sorption, the plantain leaves' pores were adhered and filled with crude oil, thus covering the bio-sorbent surface with non-regular oil dense layers (Fig. 2(b)). The covered bio-sorbent surface with non-regular oil dense layers indicated the bio-sorption of crude oil by the plantain leaves. In addition, the plantain leaves bio-sorbent after crude oil bio-sorption consisted majorly of carbon (75.18), oxygen (6.19) and manganese (5.28), respectively. Other minor amounts of elements present in the plantain leaves after bio-sorption included titanium (3.96), nickel (3.46), iron (2.12), calcium (2.02), vanadium (1.17) and potassium (0.61), respectively (Fig. 2(d) and Table 3).

3.3. Contact angle characterization

The contact angle between the leaf and the liquid (oil or water) interactions can be employed to draw conclusions about the wettability (i.e., hydrophilicity or hydrophobicity) or surface energy of the leaf. According to Jansson et al. [47], a low contact angle reveals that there is a good interaction between the liquid and the surface of the solid material, which implies good surface wettability and adhesion. It also indicates that the chemical affinity between the leaf and the liquid is high or that the leaf's surface energy is high. On the other hand, if there is a good interaction between the leaf and the liquid, a high contact angle will be obtained, indicating that the chemical affinity between the leaf and the liquid is low or that the surface energy of the leaf is low. In this study, the contact angle between the plantain leaf surface and the oil-water mixture was obtained to be $83^\circ \pm 2^\circ$, as presented in Fig. 3. This value indicates that the plantain leaf is slightly hydrophilic as well as possessing high oil adhesion.

3.4. Specific surface area, pore volume and porosity characterization

The external specific surface area and pore volume of the plantain leaves' biosorbent were determined using the BET-N_2 adsorption method. The results were obtained as follows: The specific surface area is 1008.51 m^2/g; pore volume is 0.95 cm^3/g; and the average pore diameter (size) is in the range of 1.6–3 nm. The porosity was found to be 20.7 %, which indicates that the plantain leaf is porous. The results revealed that the plantain leaves' pore diameter occurred between 0 and 50 nm, which belonged to the mesopore and micropore ranges [48]. Also, the specific surface area and the pore volume values are comparable to the specific surface area value

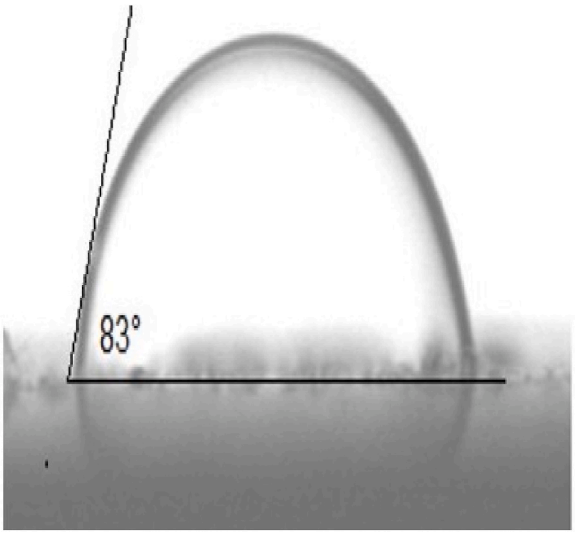

Fig. 3. Contact angle between plantain leaves-biosorbent and oil-water emulsion.

range of 798.51–1227.60 m^2/g and total pore volume range of 0.83–1.29 cm^3/g obtained by Marlín-González et al. [49] for banana leaf-derived activated carbons. Considering the fact that the pore size of the porous plantain leaves' particles falls within the mesopores and micropores size region, and with the relatively large specific surface area, the plantain leaves' biosorbent will reasonably be favorable for the biosorption of crude oil [50].

3.5. Taguchi's analysis of bio-sorptive remediation of crude oil polluted seawater

3.5.1. Effects of bio-sorption factors on bio-sorption efficiency and bio-sorption capacity

The bio-sorption efficiency and bio-sorption capacity results obtained based on L_9 (3^4) TOAT are herein presented (Table 4). For the estimation of the factor X_1 (crude oil initial concentration) effect on the output response (bio-sorption efficiency and bio-sorption capacity), the total mean of 3 observed output response at level 1 of factor X_1 was divided by 3 to get the mean output response at level 1 of factor X_1. In the same vein, the mean output responses at levels 2 and 3 were gotten. The estimated effects provided in Table 5 are graphically illustrated in Fig. 3.

The estimated individual factor's effect on bio-sorption efficiency and bio-sorption capacity of the bio-sorbent (plantain leaves) can be seen in Fig. 4.

The crude oil initial concentration effect on the oil bio-sorption efficiency and bio-sorption capacity (i.e., crude oil quantity removed per unit bio-sorbent mass) of plantain leaves is as shown in Fig. 4(a). Fig. 4(a) revealed that as the crude oil initial concentration increases there is general decline in the plantain leaves' bio-sorption efficiency and the plantain leaves' bio-sorption capacity generally increased with increasing initial concentration. This indicated that there is an inverse relationship between bio-sorption efficiency and bio-sorption capacity regarding increasing crude oil initial concentration. This observation is similar to the observation that was reported for using chemically and thermally modified coconut husk [4], plasma-treated polyethylene powder [51], oil palm fruit mesocarp fibre [52], stearic acid grafted coconut husk [19], and *Cissus populnea* leaves [25] to remove and clean-up oil from aquatic habitat. The observed decline in the plantain leaves' bio-sorption efficiency in respect to increasing crude oil initial concentration could be because the initial concentration is low, then small quantity of oil molecules is accessible for bio-sorption and since there are finite number of accessible vacant active binding sites, thus, there is rapid bio-sorption that occurs at these bio-sorbent surface active sites. As the initial concentration is increasing, then bio-sorption slowly takes place inside the pores (macro- and micro-) and the accessible vacant binding sites become filled up [4] which then induce a resistance to the concentration gradient driving force and hence results in oil desorption and a decreased oil bio-sorption [8,52,53]. Whereas the increase seen in the plantain leaves' bio-sorption capacity can be adduced to the fact that when initial concentration is low, then the ratio of the quantity of oil molecules to accessible bio-sorbent surface area is low and therefore greater quantity of oil molecules are bio-sorbed at the hydrophobic active binding sites as well as diffuses into the bio-sorbent pores [16,19,52]. With increasing initial concentration, there is an increasing concentration gradient (mass transfer) driving force that subdues the resistance to the mass transfer of oil thereby increasing the oil molecules' rate of bio-sorption and therefore resulted in an increased bio-sorption capacity [4,52].

Since there is often a variation in the temperature of water bodies (e.g. sea or ocean) with reference to location or area and change in seasons [4], its effect on plantain leaves' crude oil bio-efficiency and bio-sorption capacity was evaluated as illustrated in Fig. 4(b). It could be seen that a rise in the seawater-crude oil temperature induced a marginal increased bio-sorption efficiency and increased bio-sorption capacity. Although there was a relative decrease in bio-sorption capacity at 45 °C but was still higher than the bio-sorption capacity obtained at 25–35 °C. The marginal increase in bio-sorption efficiency due to rise in the seawater-crude oil temperature was attributed to viscosity and density of oil becoming high when temperature is low, thereby leading to the bio-sorbent pores being plugged by oil molecules and subsequently lower bio-sorption efficiency. As the temperature rises, so also the oil viscosity and density reduce (i.e., becomes low) thereby leading to an increased kinetic energy and movement of oil, rate of bio-sorption unto the bio-sorbent surface and increased diffusion rate of oil molecules into the bio-sorbent internal pores [1,20,52]. The observed decrease in bio-sorption capacity at 45 °C may be because that when temperature becomes high, the viscosity of the oil becomes low while its' water solubility increases which then makes the oil molecules to be more difficult to adsorb [8,52]. Dagde [5], Puasa et al. [2], and Eboibi et al. [52] have for the utilization of groundnut husks/plantain peels, empty bunch of oil-palm fruit, and oil palm fruit mesocarp fibre in removing oil from aquatic environment presented a similar observation of an increased oil bio-sorption efficiency and

Table 4
L_9 (3^4) TOAT layout and the obtained bio-sorption efficiency, bio-sorption capacity and S/N ratio results.

Run	Main factors				Bio-sorption efficiency (%)		Bio-sorption capacity (g/g)	
	X_1	X_2	X_3	X_4	Mean value	S/N Ratio (dB)	Mean value	S/N Ratio (dB)
L1	1	1	1	1	97.8 ± 0.32	39.81 ± 0.02	7.63 ± 0.15	17.65 ± 0.03
L2	1	2	2	2	96.3 ± 0.35	39.67 ± 0.02	3.75 ± 0.11	11.48 ± 0.05
L3	1	3	3	3	95.5 ± 0.25	39.60 ± 0.03	2.48 ± 0.10	7.89 ± 0.04
L4	2	1	2	3	93.0 ± 0.30	39.37 ± 0.01	5.44 ± 0.12	14.71 ± 0.02
L5	2	2	3	1	98.8 ± 0.30	39.90 ± 0.03	3.85 ± 0.13	11.71 ± 0.03
L6	2	3	1	2	95.6 ± 0.25	39.61 ± 0.01	11.18 ± 0.12	20.97 ± 0.04
L7	3	1	3	2	94.0 ± 0.22	39.46 ± 0.02	4.88 ± 0.10	13.77 ± 0.01
L8	3	2	1	3	90.0 ± 0.20	39.08 ± 0.04	14.04 ± 0.11	22.95 ± 0.04
L9	3	3	2	1	94.6 ± 0.35	39.52 ± 0.03	7.38 ± 0.14	17.36 ± 0.05

The values are means or average of three replicates (n = 3), values are mean ± standard deviation.

Table 5
Estimated individual factor effects on bio-sorption efficiency and bio-sorption capacity of plantain leaves.

Factors	Bio-sorption efficiency		
	Levels		
	1	2	3
Crude Oil Initial Concentration (X_1)	96.53* ± 0.25	95.80 ± 0.30	92.87 ± 0.20
Seawater-Crude Oil Temperature (X_2)	94.93 ± 0.35	95.03 ± 0.35	95.23* ± 0.25
Bio-Sorbent Dosage (X_3)	94.47 ± 0.40	94.63 ± 0.25	96.10* ± 0.40
Bio-Sorbent Particle Size (X_4)	97.07* ± 0.20	95.30 ± 0.30	92.83 ± 0.30
Bio-sorption capacity			
Crude Oil Initial Concentration (X_1)	4.62 ± 0.11	6.82 ± 0.07	8.77* ± 0.12
Seawater-Crude Oil Temperature (X_2)	5.98 ± 0.09	7.21* ± 0.09	7.01 ± 0.10
Bio-Sorbent Dosage (X_3)	10.95* ± 0.11	5.52 ± 0.08	3.74 ± 0.10
Bio-Sorbent Particle Size (X_4)	6.29 ± 0.08	6.60 ± 0.10	7.32* ± 0.08

The * indicate optimum level. The values are means of three replicates (n = 3), values are mean ± standard deviation.

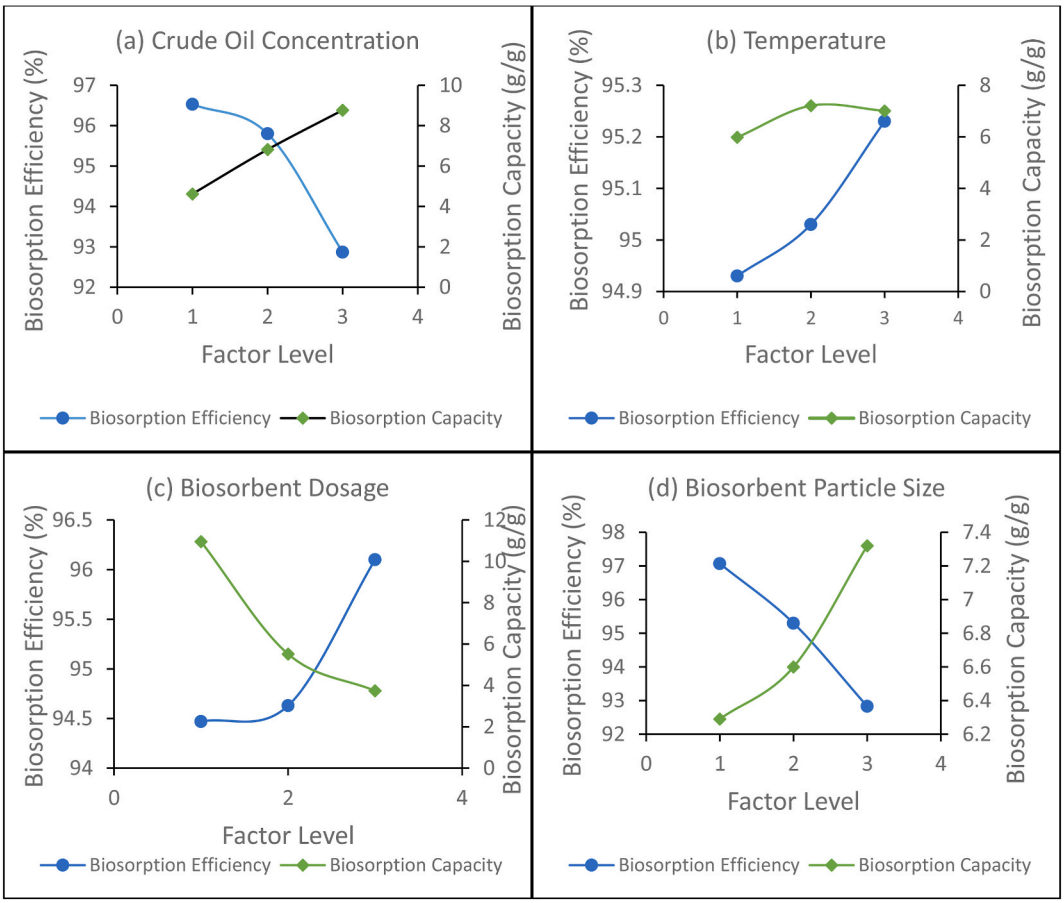

Fig. 4. Estimated individual factor effects at different factor level on bio-sorption efficiency and bio-sorption capacity of plantain leaves (a) crude oil initial concentration (b) seawater-crude oil temperature (c) bio-sorbent dosage (d) bio-sorbent particle size.

bio-sorption capacity due to temperature increase. In contrast, Olufemi and Otolorin [32] using a mango shell and an activated carbon derived-mango shell for oil bio-sorption from water have reported a decreased removal efficiency of oil due to increasing temperature. Also, Dimas and Osemeahon [8] reported a reduced oil-sorption capacity with rising temperature for sorption of oil from water utilizing *Annona senegalensis*.

Furthermore, the bio-sorption efficiency increased generally with increasing applied bio-sorbent dosage while the bio-sorbent bio-sorption capacity reduced with increment in the bio-sorbent dosage (Figure 4(c)). The observed increment in the bio-sorption efficiency in respect to increment in the bio-sorbent dosage may be that with an increase in bio-sorbent dose, there is an increment in the accessible vacant active bio-sorption binding sites together with an increased bio-sorbent contacting surface area thereby making it

easier for the penetration and uptake of oil [4,40]. In contrast, reason for the observed reduction in bio-sorption capacity could be adduced to the aggregation of reactive bio-sorption binding sites [54] of which some reactive binding sites might have been left unsaturated during the bio-sorption [3,5]. Abdelwahab et al. [3] and Dagde [5] have presented similar results of an increased oil bio-sorption efficiency and a reduced bio-sorption capacity due to increased dose of groundnut husk/plantain peels and raw palm fibers/modified palm fibers used as bio-sorbents for oil removal from water.

Fig. 4(d) illustrates the result obtained for the bio-sorbent particle size effect on both the bio-sorption efficiency and the bio-sorption capacity of plantain leaves. The result illustrates that, with an increased bio-sorbent particle size, a corresponding decreased bio-sorption efficiency and a corresponding increased bio-sorption capacity occurs. This is so, because the smaller the size of particle, the greater is the area of specific surface and the micro-pore volume which allows for less resistance to mass transfer and thus resulting in greater oil molecules' bio-sorption [23]. But as the size of particle increases (i.e., becomes large), a reduction in the area of specific surface and micro-pore volume occurs, which results in higher resistance to oil molecules mass transfer and diffusion such that majority of the particle's internal surfaces may not be utilized and thus a reduction in the quantity of oil molecules adsorbed [52,55]. A similar result using a chemically modified empty bunch of oil palm fruit and cocoa pod [16], *Ricinus communis* leaves [23], and oil palm fruit mesocarp fibre [52] for oil-sorption from aqueous phase has been presented.

3.5.2. Linear regression model and variance analysis (ANOVA)

The factorial linear regression model fit results for bio-sorption efficiency and bio-sorption capacity data are presented in Table 6.

As provided in Table 6, that the F-values of 129.90 and 25.72 gotten for the factorial linear regression model adjusted to the bio-sorption efficiency and bio-sorption capacity data are significant. There is only a 0.77 % and 0.41 % chance that "F-value" of a model which is, this large could only have occurred due to noise. The low p-value (=0.0077) attained for the linear regression model fit to the bio-sorption efficiency data proved the high adequacy and significance of the model since the p-value was less than 0.05. The correlation or determination coefficient (R^2) value (=0.9974) achieved for the bio-sorption efficiency indicated that a high correlation degree exist between the observed experimental and predicted values. The R (correlation coefficient) value of 0.9987 suggested that more than 99.87 % of the factorial linear model variance could be adduced to the factors and hence proved the high significance of the factorial linear model. Therefore, the model cannot explain the 0.13 % of the total variance for bio-sorption efficiency. The 0.9482 predicted R^2 value is in reasonable accord with the 0.9898 adjusted R^2 value obtained for the bio-sorption efficiency. S: NR is measured by 'adequate precision (AP)' and a ratio with an AP value that is above 4 is very desirable and adequate. The AP value of 37.714 attained for the bio-sorption efficiency was above 4 (i.e. AP > 4) which revealed that the S: NR for the factorial linear regression model was adequate. Therefore, the variance analysis (ANOVA) as proven by the F-test low p-value (<0.05) implied that the linear model was highly significant. Also, model terms with p-values less than 0.05 indicate their significance. For the bio-sorption efficiency, the ANOVA (Table 6) presents that the statistically significant model terms at the 95 % confidence level (P < 0.05) were X_1 (crude oil initial concentration, p-value = 0.0062), X_3 (bio-sorbent dosage, p-value = 0.0281) and X_4 (bio-sorbent particle size, p-value = 0.0051), respectively. The seawater-crude oil temperature had no significant impact on the bio-sorption efficiency. The final stage in the TOAT analysis is to predict the optimal response. After the optimal combination of factors and their levels determination through the ANOVA, S: NR and sigma value analyses, the optimal bio-sorption efficiency and the optimum bio-sorption capacity can be predicted from the following Equation (8) [38]:

$$\eta = \bar{\eta}_M + \sum_{i=1}^{k} (\eta_i - \bar{\eta}_M) \tag{8}$$

Where η_i is the S: NR mean at the optimum level; $\bar{\eta}_M$ is the total S: NR mean; and k is the number of major bio-sorption factors that significantly impacted on the response.

Table 6
ANOVA for the factorial linear regression model fitting to the bio-sorption efficiency and bio-sorption capacity data of plantain leaves in the remediation of crude oil polluted seawater.

Source	Bio-sorption efficiency SS	DF	MS	F-value	P-value	Percentage Contribution
Model	54.56	8	9.09	129.90	0.0077*	–
X_1	22.59	2	11.29	161.33	0.0062*	41.29
X_3	4.85	2	2.42	34.62	0.0281*	8.86
X_4	27.13	2	13.56	193.76	0.0051*	49.59
Error	0.14	2	0.070			0.26
Cor Total	54.70	8				100
R^2 = 0.9974; Adjusted R^2 = 0.9898; Predicted R^2 = 0.9482; Adequate Precision = 37.714						
Bio-sorption capacity						
Model	110.50	4	27.62	25.72	0.0041	
X_1	25.83	2	12.91	12.02	0.0203	
X_3	84.67	2	42.34	39.42	0.0023	
Error	4.30	4	1.07			
Cor Total	114.79	8				
R^2 = 0.9626; Adjusted R^2 = 0.9252; Predicted R^2 = 0.8106; Adequate Precision = 14.708						

N.B: SS = Sum of squares; DF = Degree of freedom; MS = Mean Square; Cor = Correlation; The * indicates significant.

Also, relying on the significant model terms, the factorial linear regression model equation obtained gives the bio-sorption efficiency (Y_{BE}) in respect of the bio-sorption factors at low and high levels: crude oil initial concentration (X_{11} and X_{13}), bio-sorbent dosage (X_{31} and X_{33}) and bio-sorbent particle size (X_{41} and X_{43}) as provided in Equation (9).

$$Y_{BE} = \rightleftarrows 95.07 + 1.47X_{11} + 0.73X_{13} - 0.60X_{31} - 0.43X_{33} + 2.00X_{41} + 0.23X_{43} \tag{9}$$

Similarly, the factorial linear regression model equation achieved for the bio-sorption capacity (Y_{BC}) in respect of crude oil initial concentration (X_{11} and X_{13}) and bio-sorbent dosage (X_{31} and X_{33}) is given in Equation (10):

$$Y_{BC} = 6.74 - 2.12X_{11} + 0.087X_{13} + 4.21X_{31} - 1.21X_{33} \tag{10}$$

Furthermore, based on Equation (9), the proposed optimization model that can be applied for predicting the optimum bio-sorption factors and optimum bio-sorption efficiency values is given in Equation (11):

$$\begin{aligned} &Maximize \rightleftarrows \rightleftarrows 95.07 + 1.47X_{11} + 0.73X_{13} - 0.60X_{31} - 0.43X_{33} + 2.00X_{41} + 0.23X_{43} \\ &Subject \rightleftarrows \rightleftarrows to: \ \rightleftarrows \rightleftarrows X_{11} + X_{13} = 1 \\ &\rightleftarrows X_{31} + X_{33} = 1 \\ &\rightleftarrows X_{41} + X_{43} = 1 \\ &\rightleftarrows X_{11}, X_{13}, X_{31}, X_{33}, X_{41}, X_{43} \in \{0, \rightleftarrows \rightleftarrows \rightleftarrows \rightleftarrows 1\} \end{aligned} \tag{11}$$

Similarly, based on Equation (10), the proposed optimization model that can be utilized for the prediction of optimum bio-sorption factors and optimum bio-sorption capacity is given in Equation (12):

$$\begin{aligned} &Maximize \rightleftarrows \rightleftarrows 6.74 - 2.12X_{11} + 0.087X_{13} + 4.21X_{31} - 1.21X_{33} \\ &Subject \rightleftarrows \rightleftarrows to: \ \rightleftarrows \rightleftarrows X_{11} + X_{13} = 1 \\ &\rightleftarrows X_{31} + X_{33} = 1 \\ &\rightleftarrows X_{11}, X_{13}, X_{31}, X_{33} \in \{0, \rightleftarrows \rightleftarrows \rightleftarrows \rightleftarrows 1\} \end{aligned} \tag{12}$$

In addition, percentage contributions (PC) of the significant factors to the bio-sorption efficiency is also presented in Table 6. Factor PC expresses the relative power of a factor to decrease or lower variation [35]. For a factor with high PC, a small perturbation or change will greatly influence the performance [56]. From the PC result in Table 6, bio-sorbent particle size (X_4) was the factor that majorly impacted on the bio-sorption efficiency (49.59 %) and was relatively followed by crude oil initial concentration (X_1) as the second ranking factor (41.29 %). The PC of bio-sorbent dosage was lower (8.86 %). The PC of the error was found to be 0.26 % which is far less than 50 %, which implied that the experiments were done under well controlled bio-sorption conditions [28]. Also, each bio-sorption factor's relative impact on the seawater-crude oil bio-sorptive remediation was further determined utilizing the variation between the values of the maximum and minimum i.e., ratios of the factor levels (i.e., sigma (δ) value) as given in Table 7.

The value of the δ (sigma) is very important for the impact ranking of factors ranging from the strongest to the weakest impact on the bio-sorption efficiency. A large δ value depicts that the factor impact or influence on the output response is strong [4,57]. Therefore, the δ values in Table 7 revealed that the bio-sorbent particle size (X_4) had a stronger influence or impact than the rest significant factors with its δ value of 0.39 relatively being the highest. This was relatively followed by crude oil initial concentration (X_1) with δ = 0.34 and bio-sorbent dosage (X_3, δ = 0.15). The seawater-crude oil temperature (X_2) impact on the bio-sorption efficiency is very weak (δ = 0.03) and thus, not significant. Also, it was seen that the significant bio-sorption factors ranking sequence achieved from the PC usage and the δ values was consistent with the factors' ranking using the p-values in the ANOVA (Table 6). That is, bio-sorption efficiency was mostly and positively impacted by bio-sorbent particle size (p = 0.0051) and then followed by initial concentration (p = 0.0062) and bio-sorbent dosage (p = 0.0281).

Table 7
Mean S: NR response for the crude oil bio-sorption efficiency and bio-sorption capacity of plantain leaves.

Factors	Bio-sorption efficiency			
	Levels			δ = Maximum – Minimum
	1	2	3	
Crude oil initial concentration (X_1)	39.69* ± 0.02	39.63 ± 0.01	39.35 ± 0.02	0.34
Seawater-crude oil temperature (X_2)	39.55 ± 0.03	39.55 ± 0.01	39.58* ± 0.03	0.03
Bio-sorbent dosage (X_3)	39.50 ± 0.02	39.52 ± 0.02	39.65* ± 0.02	0.15
Bio-Sorbent particle Size(X_4)	39.74* ± 0.01	39.58 ± 0.03	39.35 ± 0.01	0.39
Total mean (S: NR) $\bar{\eta}_M$	39.56 ± 0.02			
Bio-sorption capacity				
Crude oil initial concentration (X_1)	12.34 ± 0.02	15.80 ± 0.01	18.03* ± 0.03	5.69
Seawater-crude oil temperature (X_2)	15.38 ± 0.02	15.38 ± 0.03	15.41* ± 0.02	0.03
Bio-sorbent dosage (X_3)	20.52* ± 0.01	14,52 ± 0.02	11.12 ± 0.01	9.40
Bio-sorbent particle size (X_4)	15.57* ± 0.03	15.41 ± 0.01	15.18 ± 0.02	0.39
Total mean (S:NR) $\bar{\eta}_M$	15.39 ± 0.01			

*Optimum level. The values are means of three replicates (n = 3), values are mean ± standard deviation.

3.5.3. Crude oil polluted seawater bio-sorptive remediation: Parametric optimization

The experimental bio-sorptive remediation results presented in section 3.1 (Table 4) showed that the maximum bio-sorption efficiency of 98.8 % was achieved in experimental run L5 where the experimental bio-sorption conditions were combination of the levels X_{12}, X_{22}, X_{33}, and X_{41}; that is: initial concentration (11.7 g/L), seawater-crude oil temperature (35 °C), bio-sorbent dosage (3 g) and bio-sorbent particle size (1.18 mm) than the levels X_{11}, X_{21}, X_{31} and X_{41} (Run L1). In contrast, minimum bio-sorption efficiency of 90 % was achieved utilizing factors' levels combination of X_{13}, X_{22}, X_{31}, and X_{43} (Run L8) which are: crude oil initial concentration (15.6 g/L), seawater-crude oil temperature (35 °C), bio-sorbent dosage (1 g) and bio-sorbent particle size (4.72 mm). Nonetheless, using the calculated mean S/N ratio for the various significant factors' levels (Table 7), levels X_{11}, X_{33}, and X_{41} were selected as the maximum or optimum set of levels of the different significant bio-sorption factors to maximize the bio-sorption efficiency (Fig. 5(a)&b). Fig. 5 illustrates the plot for the S: NR where the S: NR's total mean value is depicted by the dashed line. Fundamentally, the better is the bio-sorption efficiency when the S: NR ratio is large, However, using the TOAT (i.e., the S: NR concept), the optimal combination of factors and their levels were obtained to be $X_{11}X_{33}X_{41}$ for the bio-sorption efficiency and $X_{13}X_{31}$ for the bio-sorption capacity, while the predicted optimum bio-sorption efficiency and the optimum bio-sorption capacity at these different factors' levels combination was 99.56 % and 12.98 g/g, respectively. Furthermore, using the model Equation (11) that was proposed, solutions to the equation are: $X_{11} = X_{33} = X_{41} = 1$ and $X_{13} = X_{31} = X_{43} = 0$.

Therefore, the predicted optimal bio-sorption conditions for optimum or maximum bio-sorption efficiency were obtained to be crude oil initial concentration, 7.8 g/L (factor X_1 level 1), bio-sorbent dosage, 3 g (factor X_3 level 3) and bio-sorbent particle size, 1.18 mm (factor X_4 level 1) while at these optimum conditions, the predicted maximum or optimum bio-sorption efficiency achieved was 98.11 %. In a similar mode, utilizing the proposed model Equation (12), the equation solutions are: $X_{11} = X_{33} = 0$ and $X_{13} = X_{31} = 1$. Thus, the predicted optimal bio-sorption conditions for optimum bio-sorption capacity were initial crude oil concentration, 15.6 g/L (level 3 of factor X_1) and bio-sorbent dosage, 1 g (level 1 of factor X_3) and at these optimum conditions, the predicted optimum bio-sorption capacity obtained was 11.04 g/g. In addition, numerical-desirability function optimization technique (N-DOT) tool of Design-Expert software (version 13) was further conducted to predict the optimum bio-sorption factors required for crude oil-seawater remediation.

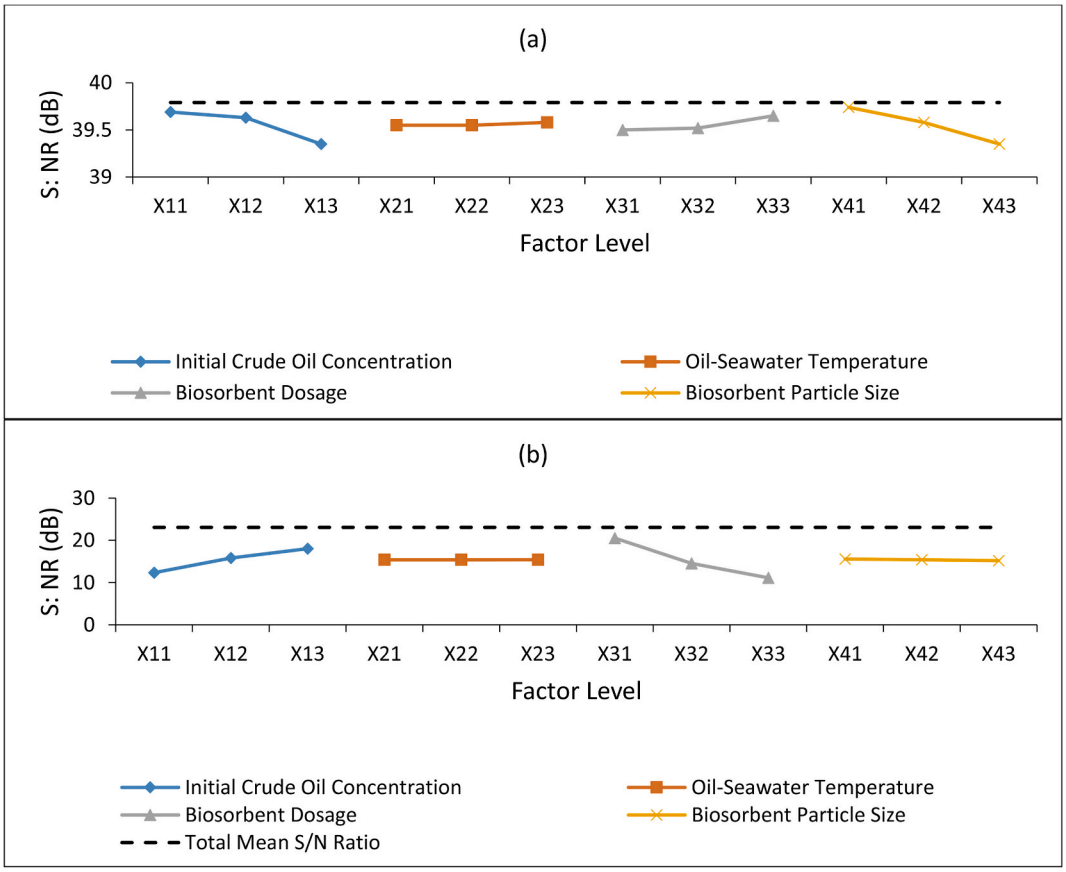

Fig. 5. (a) S: NR plot for crude oil bio-sorption efficiency of plantain leaves at different levels of factors. (b) S: NR plot for bio-sorption capacity of plantain leaves at different levels of factors.

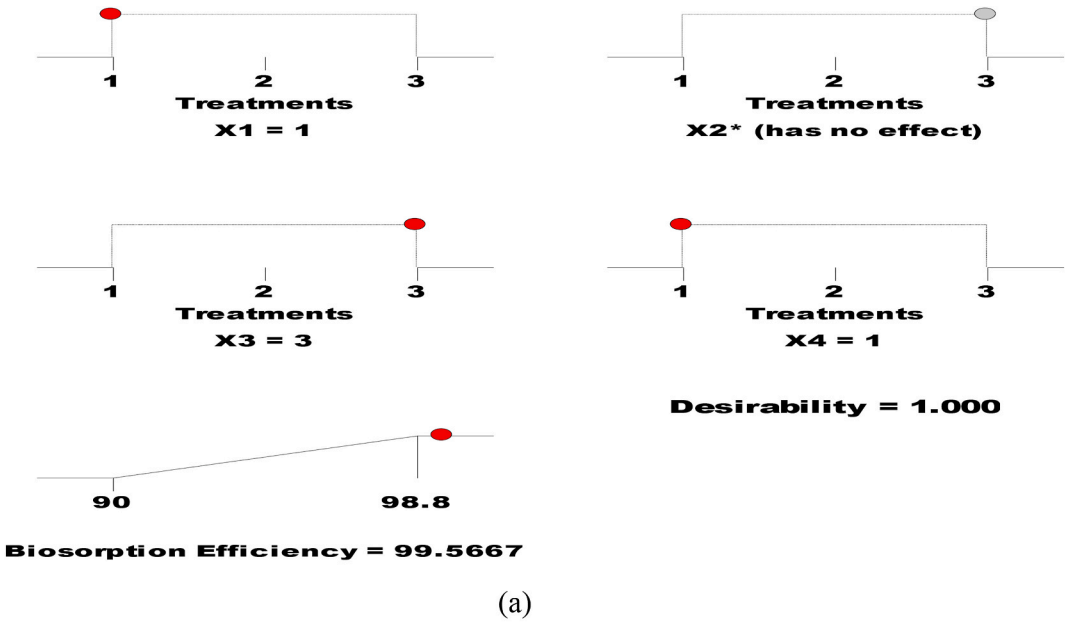

(a)

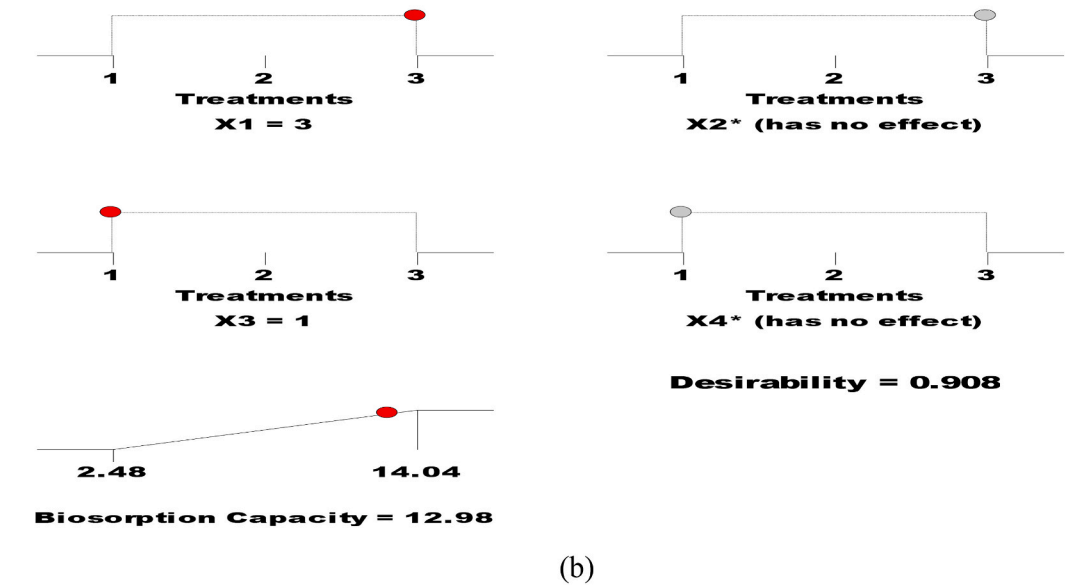

(b)

Fig. 6. (a) Ramp desirability plot for crude oil bio-sorption efficiency optimization (b) Ramp desirability plot for the bio-sorption capacity optimization.

Table 8
Confirmatory/validation experimental results.

	Optimal bio-sorption parameters				
	Predicted[A]	Predicted[B]	Predicted[C]	Experimental	% Error
Level	$X_{11}X_{33}X_{41}$	$X_{11}X_{33}X_{41}$	$X_{11}X_{33}X_{41}$	$X_{11}X_{33}X_{41}$	
Bio-sorption efficiency (%)	98.11	99.57	99.57	99.05 ± 0.15	0.95^{A}; -0.52^{BC}
S:NR (dB)	39.83	39.96	39.96	39.92 ± 0.05	
Level	$X_{13}X_{31}$	$X_{13}X_{31}$	$X_{13}X_{31}$	$X_{13}X_{31}$	
Bio-sorption capacity (g/g)	11.04	12.98	12.98	12.82 ± 0.08	14^{A}; -1.25^{BC}
S:NR (dB)	20.86	22.27	22.27	22.16 ± 0.04	

[A]Proposed optimization model; [B]Taguchi optimization technique; [C]N-DOT.

The predicted theoretical optimum values for initial crude oil concentration (X_1), bio-sorbent dosage (X_3) and bio-sorbent particle size (X_4) were obtained to be: X_{11} (7.8 g/L), X_{33} (3 g) and X_{41} (1.18 mm) which would result in the predicted optimum bio-sorption efficiency of 99.57 % having a desirability index of 1.000 (Fig. 6(a)&b).

These predicted optimum conditions were found to also be in accord with the optimum set of factors' levels achieved from both the proposed optimization model and the Taguchi optimization technique (i.e., Equation (8): mean S: NR analysis). The predicted theoretical bio-sorption capacity was validated or confirmed by conducting a confirmatory or validation experiment under the predicted optimum levels of the significant bio-sorptive remediation factors. The experiment was repeated 3 times (triplicate). The results are shown in Table 8.

Utilizing Equation (13) [58], the percentage errors (%Error) that exist between the predicted or theoretical bio-sorption capacity, bio-sorption efficiency, and their corresponding actual confirmed experimental bio-sorption efficiency and bio-sorption capacity values were calculated.

$$\%Error = \frac{Actual\rightleftarrows Confirmed\rightleftarrows Experimental\rightleftarrows Value - \Pr edicted\rightleftarrows Value}{Actual\rightleftarrows Confirmed\rightleftarrows Experimental\rightleftarrows Value} \times 100 \quad (13)$$

As indicated in Table 8, the confirmed bio-sorption efficiency of 99.05 % and bio-sorption capacity of 12.82 were obtained with a mean S: NR of 39.92 dB and 22.16 dB, respectively. A value of 0.95 %, −0.52 % and −0.52 % was the respective computed %Error between the actual confirmed bio-sorption efficiency value and the predicted bio-sorption efficiency values garnered from the applied proposed optimization method, the Taguchi optimization technique and the N-DOT, thus showing that there exist no significant difference between them. Meanwhile, the %Errors between the actual confirmed bio-sorption capacity and the predicted bio-sorption capacity values achieved using the proposed optimization method, Taguchi optimization technique and the N-DOT were, 14 %, −1.25 % and −1.25 %, respectively. Hence, there exists no significant variation between the predicted values and the actual confirmed value.

3.6. Regeneration/reusability of plantain leaves biosorbent

In this study, the used biosorbent loaded with crude oil was regenerated using hot water at 100 °C (thermal method) [59]. The spent biosorbent was several times rinsed with hot water to desorb crude oil from it. The rinsed biosorbent was then dried and re-used for oil biosorption to evaluate its biosorption efficiency and biosorption capacity after regeneration. Five regeneration or reusability cycles were conducted, and the results are illustrated in Fig. 7(a)&b.

The results revealed that the biosorption efficiency decreased from 99.05 % to a level of 49.55 % after the fifth cycle, while the biosorption capacity decreased from 12.82 g/g to 6.46 g/g. Thus, the decrease in biosorption efficiency and biosorption capacity did not approximately exceed 50 % of the initial value after five biosorption cycles. Based on Table 9, the reusability of plantain leaves' bio-sorbent was similar to bio-sorbents like raw luffa [60], Lawsonia leaves [26], orange peel [61], barley straw [62] and pineapple leaves [22]. Nevertheless, the plantain leaves reusability was limited when compared to some bio-sorbents whose reusability cycles were up to 8–15 including *Annona senegalensis* fiber (wild custard apple) [8] and banana peel [63].

3.7. Comparison of plantain leaves' oil biosorption efficiency and biosorption capacity

Table 9 shows the comparison of the plantain leaves' crude oil biosorption efficiency and biosorption capacity with the oil removal efficiency and biosorption capacity of selected lignocellulosic biosorbents.

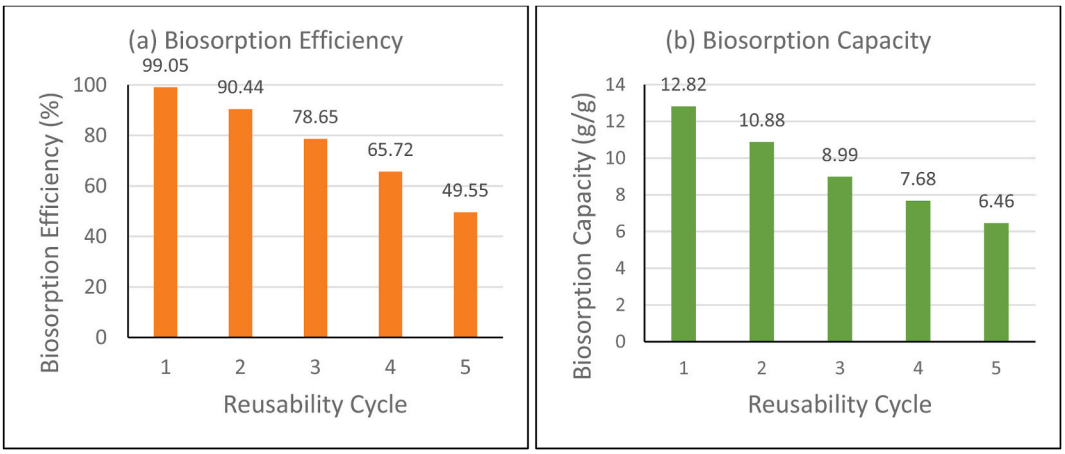

Fig. 7. Reusability of plantain leave as crude oil biosorbent conducted at crude oil initial concentration of 7.8 g/L, seawater-crude oil temperature of 30 °C, bio-sorbent dosage of 3 g and bio-sorbent particle size of 1.18 mm. (a) biosorption efficiency (b) biosorption capacity.

Table 9
Comparison of plantain leaves' oil bio-sorption efficiency and bio-sorption capacity with selected bio-based (lignocellulose) bio-sorbents.

Type of Biosorbent	Type of oil	BE (%)	BC (g/g)	RC	Ref
Luffa fibre	Crude oil	44	10	3	60
Sugarcane leaves/bagasse	Crude oil	N/A	5.5 and 6.6	N/A	64
Banana peel	Crude oil	N/A	5–7	10–15	63
Barley straw	Crude oil	N/A	6.5–12	3	62
Rice husk	Crude oil	N/A	15	N/A	65
Date palm fibers	Crude oil		22.73	N/A	3
Orange peel	Crude oil	N/A	3–5	5	61
Acetylated cocoa pod fibre/acetylated oil palm empty fruit bunch	Crude oil	N/A	8 and 7	N/A	16
Groundnut husk/plantain peels	Crude oil	85.81/89.6	0.054/0.056	N/A	5
Plantain pseudo stem fiber	Crude oil	94.7/98.56	0.054	N/A	42
Neem leaves	Crude oil	70.87–80.5		N/A	24
Raw/acetylated coconut husk	Crude oil	50/84.2	5 and 8.42	N/A	4
Annona senegalensis fiber (wild custard apple)	Crude oil		5.25–7.12	8	8
Oil palm fruit mesocarp fibre	Crude oil	97.25	12.66	N/A	52
Walnut shells and Date pits	Oil	80 and 87	–	N/A	66
Modified oil palm leaves	Oil	N/A	1.176	N/A	41
Coconut coir	Oil	N/A	0.360	N/A	67
Corncobs		N/A	5–7	N/A	13
Fatty acid-modified pomelo peels	Diesel oil and Lubricating oil	N/A	5.96–11.49/7.59–14.17	N/A	68
Moss *(Ceratodon purpureus)*	Engine oil	N/A	25.5	N/A	69
Raw Spent tea leaves and Oleic modified spent leaves		N/A	1.8 and 2.267	N/A	27
Raw pineapple leaves and Fatty acid-esterified pineapple leaves	Oil	N/A	0.0356 and 0.107–0.1389	4	22
Lawsonia leaves		N/A	1.60	4	26
Cissus Populnea leaves		N/A	20.4	N/A	25
Plantain leaves	Crude oil	99.05 %	12.82	5	Present study

Note: N/A = Not Available; RE = Biosorption Efficiency; BC = Biosorption Capacity; RC = Reusability Cycle and Ref = Reference.

As shown in Table 9, the oil biosorption capacity values for plantain leaves biosorbent (12.82 g/g) reported in this present study are relatively comparable to the oil sorption capacity of barely straw (6.5–12 g/g) [62], rice husk (15 g/g) [65], fatty acid-modified pomelo peel (11.49 and 14.17 g/g) [68], raw luffa (10 g/g) [60], and oil palm (*Elaeis guineensis*) fruit mesocarp fibre (12.66 g/g) [52], while it is greater than the reported values for modified oil palm leaves (1.176 g/g) [41], corncobs (5–7 g/g) [13], raw pineapple leaves (35.59 mg/g) and fatty acid-esterified pineapple leaves (107.67–138.89 mg/g) [22], groundnut husk (0.054 g/g) and plantain peels (0.056 g/g) [5] coconut coir (0.360 g/g) [67], raw sugarcane bagasse (6.6 g/g) [64], banana peel powder (5–7 g/g) [63], acetylated cocoa pod fibre (8 g/g) and acetylated oil palm empty fruit bunch (7 g/g) [16], orange peel (3–5 g/g) [61], raw coconut husk (5 g/g) and acetylated coconut husk (8.42 g/g) [4], raw spent tea leaves (1.8 g/g) and oleic modified spent leaves (2.267 g/g) [27], plantain pseudo-stem fibers (54.35 mg/g) [42] and lawsonia leaves (1.60 g/g) [26]. In addition, the biosorption efficiency value (99.05 %) reported in this study is comparable with the oil removal efficiency reported for plantain pseudo-stem fibers (98.56 %) [42] and oil palm fruit mesocarp fibre (97.25 %) [52], whereas, it is relatively greater than the values reported for groundnut husk (85.81 %) and plantain peels (89.56 %) [5], neem leaves (70.87–80.5 %) [24], walnut shell (80 %) and date pits (87 %) [66], raw coconut husk (50 %) and acetylated coconut husk (84.2 %) [4]. The fact that plantain leaves biosorbent has exhibited good oil biosorption efficiency and biosorption capacity compared to other lignocellulosic biosorbents, the biosorption capacity value reported in this study are lower to the oil sorption capacity values that have been reported for palm fiber (22.73 g/g) [63], moss *(Ceratodon purpureus)* (25.5 g/g) [69], and *Cissus Populnea* Leaves (20.4 g/g) [25].

3.8. Crude oil bio-sorptive remediation isotherms' modelling

Different types of isotherm models have been developed to describe equilibrium relationship that exists between the bio-sorbent and sorbate [4,28,42,54]. Langmuir, Freundlich, and Temkin, which are two-parameter isotherm models were utilized to succinctly describe the equilibrium bio-sorptive remediation data.

3.8.1. The Langmuir isotherm model

This model describes the gradual increasing occupation of the limiting number of homogeneously spread identical reactive sites present on the entire bio-sorbent surface area with mono or single layer of the sorbate until no further adsorption or sorption can take place [42]. The linearized model form is expressed as given in Equation (14) [42]:

$$\frac{C_e}{q_e} = \frac{1}{q_{\max} a} + \frac{C_e}{q_{\max}} \tag{14}$$

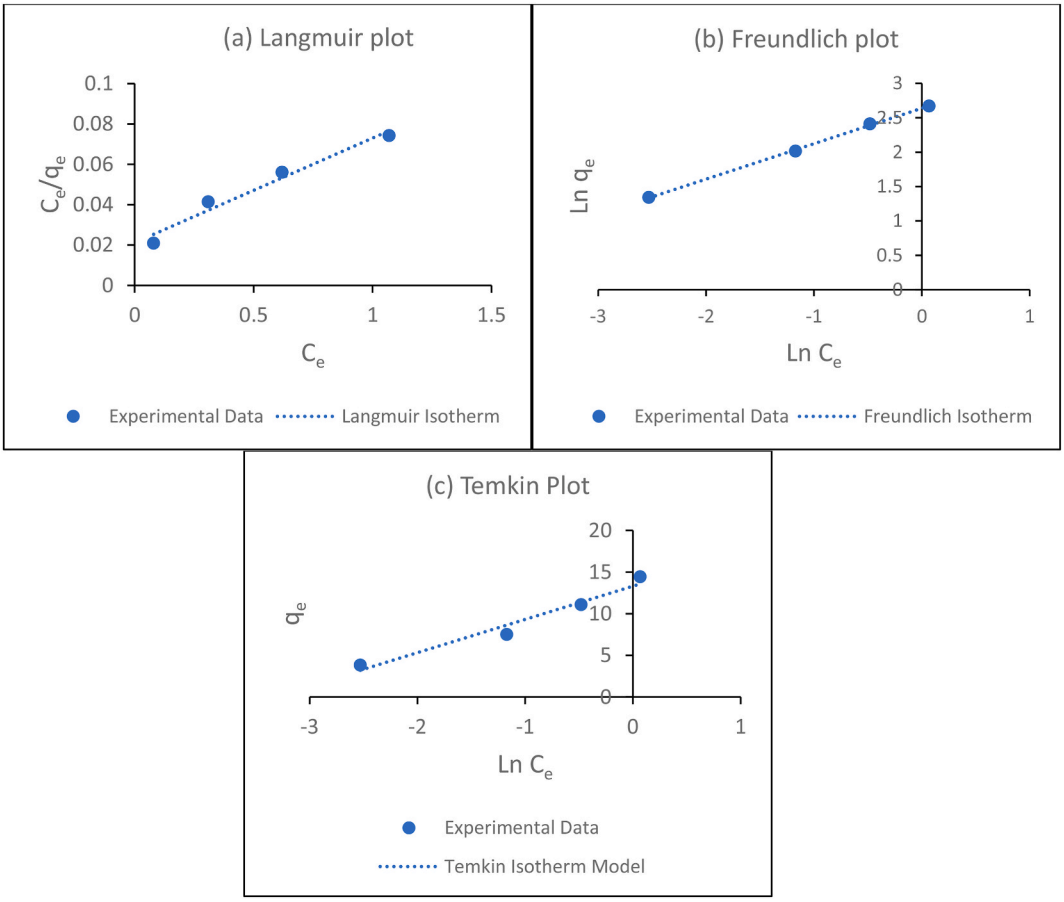

Fig. 8. Bio-sorption isotherm models fitting to the equilibrium plantain leaves-crude oil bio-sorptive remediation data obtained at conditions of different crude oil initial concentration, constant seawater-crude oil temperature (30 °C), bio-sorbent dosage (3 g), and bio-sorbent particle size (1.18 mm). (a) Langmuir isotherm model linear regression fitting. (b) Freundlich isotherm model linear regression fitting. (c) Temkin isotherm model linear regression fitting.

Table 10
Estimated values of the bio-sorption isotherm parameters and R^2 for the crude oil-seawater system bio-sorptive remediation by plantain leaves (value of parameters obtained at conditions of different crude oil initial concentration, constant seawater-crude oil temperature (30 °C), biosorbent dosage (3 g), and biosorbent particle size (1.18 mm).

Isotherm models	Isotherm constant parameters		Correlation coefficient
	Name	Value	R2
Langmuir Isotherm	$q_{max}(g/g)$	19.31	0.9673
	$a(L/g)$	2.44	
Freundlich Isotherm	$K_f(g/g)(L/g)$	13.99	0.9991
	$1/n$	0.516	
Temkin Isotherm	$A(L/g)$	28.02	0.9600
	B	3.993	
	$b_T(kJ/mol)$	0.622	

where q_{max} (maximum bio-sorption capacity, g/g) and a (bio-sorption affinity indicator or bio-sorption energy, L/g) are Langmuir constants. They were determined from the slope and intercept of the linear regression plot of C_e/q_e vs. C_e as shown in Fig. 8(a). The estimated or determined values of the constants are provided (Table 10). Fig. 8(a) revealed that the equilibrium bio-sorption data adequately adjusted well to the Langmuir isotherm model (with R^2 value = 0.9673, Table 10). Table 10 shows the Langmuir constant, a to be 2.44 L/g while the q_{max} to be 19.31 g/g. It was reported that when Langmuir constant a is above zero (i.e., $a > 0$), then the adsorption or sorption system is favorable [54]. Since the constant "a" was seen to be greater than zero (>0), hence, the bio-sorption of the crude oil from the seawater was much favorable. The plantain leaves' q_{max} value of 19.31 g/g was relatively comparable with the q_{max} values of 15.3 g/g and 15.06–16.84 g/g respectively gotten for oil-sorption from water using esterified coconut coir [70] and

chemically and thermally modified coconut husk [4].

3.8.2. The Freundlich isotherm model

The model is usually employed to describe the occurrence of non-ideal sorption or adsorption in a heterogeneous sorbent/adsorbent surface that has independent and non-equivalent reactive binding sites [4]. The linearized logarithmic model form is as provided in Equation (15):

$$Ln\rightleftarrows q_e = Ln\rightleftarrows K_f + \left(\frac{1}{n}\right) Ln\rightleftarrows C_e \tag{15}$$

The K_f and n are Freundlich isotherm constants. The K_f roughly denotes the bio-sorption or adsorption capacity (g/g) and n is an empirical constant that denotes the bio-sorption intensity. The two constants (K_f and $1/n$) were derived from the slope and intercept of the linearized plot, $Ln\rightleftarrows q_e$ vs. $Ln\rightleftarrows C_e$ (Fig. 8 (b)). The estimated or determined values of both constants are presented (Table 10). Fig. 8 (b) illustrated that the equilibrium bio-sorption data adjusted adequately to the Freundlich isotherm model relatively having a high R^2 value of 0.9991. Table 10 reveals that the Freundlich constant K_f was 14.00 g/g while the empirical constant $1/n$ constant was 0.516. Also, it was reported that, for a favorable adsorption or bio-sorption, the value of $1/n$ should be less than one (i.e., $1/n < 1$) or that the value of "n" should be above one but less than ten (i.e., $1 < n < 10$) [4,9]. The smaller or lower the 1/n value, the greater is the binding affinity that will exist between the sorbate and the bio-sorbent or adsorbent [4,71]. Therefore, the $1/n$ value of 0.516 or the n value of 1.94 gotten for the utilization of plantain leaves as bio-sorbent denotes a favorable crude oil bio-sorption. The $1/n$ value, 0.516

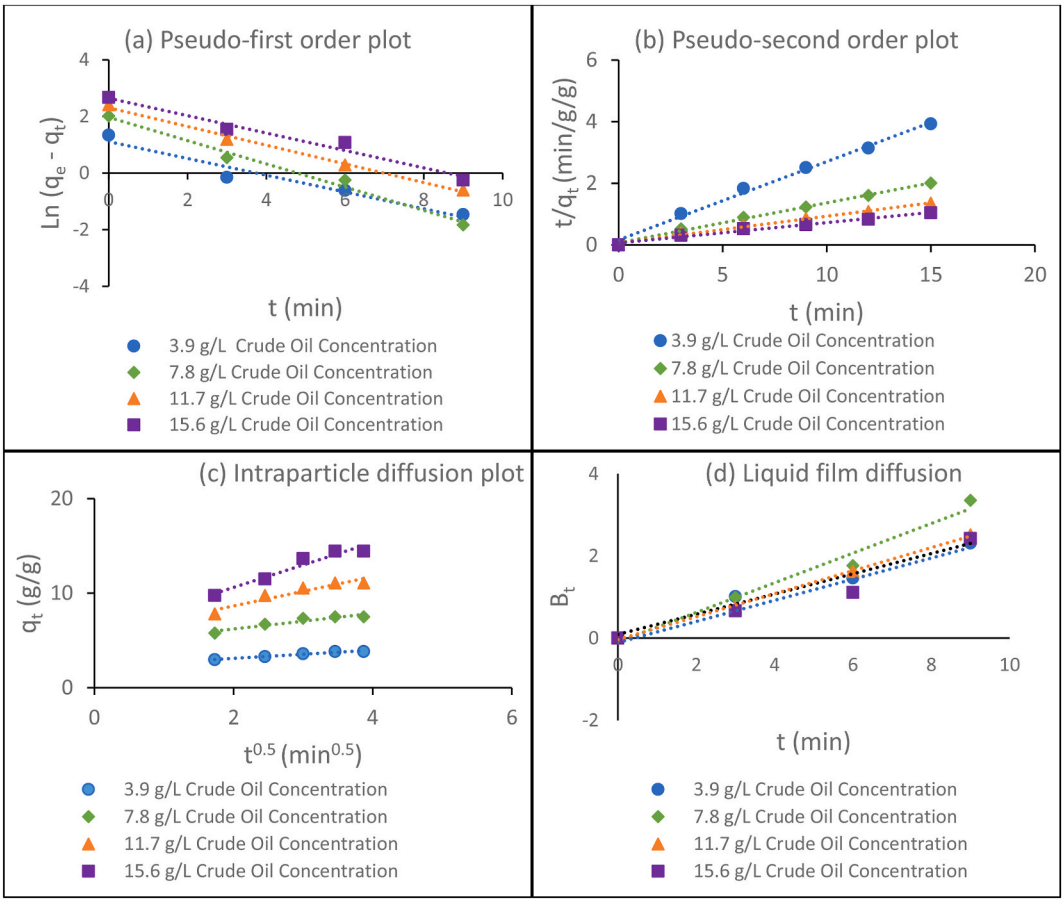

Fig. 9. (a) Pseudo-first-order kinetics adjusted to the plantain leaves' crude oil bio-sorptive kinetic data obtained at various crude oil initial concentration, constant seawater-crude oil temperature (30 °C), biosorbent dosage (3 g), and biosorbent particle size (1.18 mm). (b) Pseudo-second-order kinetics adjusted to the plantain leaves' crude oil bio-sorptive kinetic data obtained at various crude oil initial concentration, constant seawater-crude oil temperature (30 °C), biosorbent dosage (3 g), and biosorbent particle size (1.18 mm). (c) Weber-Morris intra-particle diffusion model adjusted to the plantain leaves' crude oil bio-sorptive kinetic data obtained at various crude oil initial concentration, constant seawater-crude oil temperature (30 °C), biosorbent dosage (3 g), and biosorbent particle size (1.18 mm). (d) Boyd et al. model adjusted to the plantain leaves' crude oil bio-sorptive kinetic data obtained at various crude oil initial concentration, constant seawater-crude oil temperature (30 °C), biosorbent dosage (3 g), and biosorbent particle size (1.18 mm).

obtained for plantain leaves as bio-sorbent for crude oil bio-sorption was relatively comparable with the $1/n$ values, 0.468 and 0.49–0.575 that were respectively gotten for the usage of raw coconut husk [4] and chitosan-g-octanal schiff base [9] in the oil-sorption from water.

3.8.3. The Temkin isotherm model

Application of the model assumes that the coverage of the bio-sorbent surface is a function of the bio-sorption free energy [54]. The Temkin model, expressed in a linear logarithmic form (Equation (16)):

$$q_e = B \ln A + B \ln C_e \tag{16}$$

where, $B = RT/b_T$. B is an indicator of the heat of sorption; b_T is a constant; T is absolute temperature (K); R is gas constant (8.314×10^{-3} kJ mol^{-1} K^{-1}); and A (L/min) is the equilibrium binding constant which connotes the maximum binding energy. From the intercept and slope of the linear regression plot of q_e vs. ln C_e (Fig. 8(c)), A and B can be computed. The A, B and b_T values determined from the plot are provided in Table 10. The plot in Fig. 8(c) indicated that the equilibrium crude oil bio-sorption data adjusted adequately to the Temkin model having a relatively high R^2 value of 0.9600. The Temkin constant, b_T was gotten to be 0.622. This value was evaluated to be less than 8 kJ/mol suggesting the weak interaction that exists between the molecules of crude oil and the plantain leaves bio-sorbent. Hence, with the b_T value < 8 kJ/mol, the plantain leaves-crude oil bio-sorption process can be assessed to be of physical bio-sorption mechanism [4,54].

Thus, the three isotherm models of Langmuir, Freundlich, and Temkin applied to the equilibrium bio-sorptive remediation data adjusted adequately with high R^2 values greater than 0.90. However, the plantain leaves-crude oil bio-sorptive remediation process could best be described by Freundlich isotherm model since it relatively presented a higher R^2 value of 0.9991. This then implied that the bio-sorption of crude oil by the plantain leaves bio-sorbent took place at the heterogeneous reactive binding sites with non-uniform or heterogeneous energy distribution. The result is in accord with the results that have been presented for leaves and roots of *Pistia stratiotes* [72] and chemically/thermally modified coconut husk used in oil-water system clean-up [4].

3.9. Kinetic modelling of the bio-sorptive crude oil polluted-seawater remediation

In ascertaining the crude oil bio-sorption mechanisms, the kinetic data obtained by calculating the bio-sorbent's oil bio-sorption capacity at different remediation time or period were analyzed utilizing the Lagergren pseudo-first order and pseudo-second order. In addition, in any bio-sorption processes, it is essential to ascertain the sorbate transfer or transport extent from the whole liquid to the bio-sorbent surface or at the bio-sorbent and liquid interface [73,74] and its diffusion into the solid bio-sorbent interior. The slowest rate step that occurs during the bio-sorption process determines the process controlling-rate step. Thus, there are different models for mass transfer or diffusion that can be utilized to determine this controlling-rate step and some of these models include Weber-Morris intra-particle diffusion model and Boyd et al. film and particle diffusion model [74]. These diffusion models were applied to ascertain the controlling-rate step of the crude oil bio-sorptive remediation process.

3.9.1. Lagergren pseudo-first-order kinetic model

This model assumes that the sorbate uptake rate at the sorption binding sites is directly proportional to the amount or number of unoccupied sorption sites [20]. The Lagergren pseudo first-order kinetic model equation (Equation (17)) as provided in the linear form [4,28,74]:

$$\ln(q_e - q_t) = \ln q_{theo} - k_1 t \tag{17}$$

Where, q_e = experimental equilibrium biosorption capacity (g/g); q_{theo} = theoretical equilibrium biosorption capacity (g/g); and k_1 = bio-sorptive rate constant (min^{-1}). The values of q_{theo} and k_1 constants were correspondingly gotten from the intercept and slope of $\ln(q_e - q_t)$ vs t plot (Fig. 9(a)). The values are provided in Table 11. Fig. 9(a) displayed that the pseudo-first-order kinetic model adjusted well to the oil bio-sorptive remediation kinetic data (at various initial crude oil concentrations) with relatively high R^2 values that ranged from 0.9515 to 0.9935 (Table 11).

Table 11 indicated that the estimated theoretical q_e (q_{theo}) is not close to the experimentally observed q_e and that generally the bio-sorptive rate constant (k_1) increased as initial concentration of the crude oil increased. The reason for the bio-sorptive rate constant (k_1) was adduced to the fact that, at lower concentration, the competition for the bio-sorbent surface reactive binding or sorption sites is low but at higher crude oil initial concentration, there is higher competition for the bio-sorbent surface reactive sorption sites which results in a higher rate of bio-sorption [54].

3.9.2. Pseudo-second-order kinetic model

This model fundamentally assumes that chemical sorption or bio-sorption is the rate-determining step [4] and that the rate of bio-sorption onto the sorption binding sites is related to the square of the accessible unoccupied sorption sites [28]. The pseudo-second-order kinetic model equation is expressed in the linear form (Equation (18)) [4,28,74]:

$$7\frac{t}{q_t} = \frac{1}{k_2 q_{theo}^2} + \frac{t}{q_{theo}} \tag{18}$$

Table 11
Pseudo-first-order, pseudo-second-order, Weber-Morris intra-particle diffusion and Boyd et al. diffusion kinetic parameters and coefficients of determination obtained for the bio-sorptive remediation of crude oil polluted seawater by plantain leaves (values obtained at conditions of different crude oil initial concentration, constant seawater-crude oil temperature (30 °C), bio-sorbent dosage (3 g), and bio-sorbent particle size (1.18 mm)).

Kinetic Model	Parameters	Crude oil initial concentration (g/L)			
		3.9	7.8	11.7	15.6
Pseudo first-order kinetics	k_1 (min^{-1})	0.297	0.411	0.330	0.307
	q_e (theo) (g/g)	3.03	7.16	10.04	14.05
	q_e (exp) (g/g)	3.82	7.49	11.08	14.43
	R^2	0.9515	0.9855	0.9935	0.9716
Pseudo second-order kinetics					
	k_2 (g/g/min)	0.396	0.239	0.116	0.065
	q_e (theo) (g/g)	3.93	7.72	11.53	15.20
	q_e (exp) (g/g)	3.82	7.49	11.08	14.43
	h	6.12	14.24	15.42	15.02
	R^2	0.9937	0.9957	0.9921	0.9845
Weber-Morris Intraparticle Diffusion					
	K_{w-m} (g/g.$min^{-1/2}$)	0.434	0.830	1.549	2.374
	C	2.236	4.550	5.554	5.862
	D_{id} (cm^2/s)	1.05×10^{-6}	1.00×10^{-6}	1.58×10^{-6}	2.20×10^{-6}
	R^2	0.9644	0.9000	0.9061	0.9393
Boyd et al. Film Diffusion Model					
	D_{Feff} (cm^2/s)	1.50×10^{-6}	2.17×10^{-6}	1.67×10^{-6}	1.50×10^{-6}
	R^2	0.9811	0.9760	0.9985	0.9480

Where k_2 = bio-sorptive rate constant of second order bio-sorption ($gg^{-1}min^{-1}$). The k_2 and q_{theo} parameters were computed from t/q_t vs. t linearized plot (Figure 8(b)). Using Equation (19), the initial bio-sorptive rate, h (g g^{-1} min^{-1}) was estimated [54].

$$h = k_2 q_{theo}^2 \tag{19}$$

The plot in Fig. 9(b) has shown that the pseudo-second-order kinetic model adequately adjusted to the oil bio-sorptive remediation kinetic data having a high R^2 values that ranged from 0.9845 to 0.9957. The estimated values of the pseudo-second-order kinetic constants are presented in Table 11. It could be seen that, generally the second-order bio-sorptive rate constant (k_2) decreased with increasing initial concentration of the crude oil, while the initial bio-sorptive rate (h) increased with rising or incremental crude oil initial concentration. Eweida et al. [9] reported a similar observation for the utilization of chitosan and chitosan-g-Octanal schiff in the removal of oil from water. The decrease in k_2 due to incremental crude oil initial concentration seems to suggest that the crude oil-seawater bio-sorptive remediation by plantain leaves was more favorable with lower concentration. Nonetheless, the reason for h increase due to incremental initial concentration may be attributed to the increased concentration gradient which results in an increased or higher driving force responsible for overcoming the crude oil mass transfer opposition between the seawater and the solid bio-sorbent [54].

3.9.3. Weber-Morris intra-particle and Boyd et al. (film and particle) diffusion models

The Weber-Morris intra-particle diffusion model equation (Equation (20)) [74,75]:

$$q_t = K_{w-m} t^{1/2} + C \tag{20}$$

Where C (g/g) = interfacial film resistance or boundary layer impact and K_{w-m} = Weber-Morris intra-particle diffusion rate constant (g g^{-1}.$min^{-1/2}$). From the intercept and slope of q_t vs $t^{1/2}$ linearized plot, C and K_{w-m} can correspondingly be estimated. The large value of C (intercept) reveals the contribution of surface bio-sorption in the controlling-rate step. If the C or intercept value is large, then the surface bio-sorption contribution in the controlling-rate step will also be large. There is a relationship existing between the intra-particle diffusion rate constant (K_{w-m}) and the intra-particle diffusivity (D_{id}, cm^2/s) which is depicted by Equation (21) [74]:

$$K_{w-m} = \left(\frac{3q_e}{d_p}\right)\sqrt{\frac{D_{id}}{\pi}} \tag{21}$$

Where d_p = bio-sorbent particle diameter (mm) and q_e = experimental equilibrium bio-sorption capacity (g/g). If from the q_t vs $t^{1/2}$ plot, a linearized regression fit through the origin is achieved, then the bio-sorption process is confirmed to be diffusion process control [75].

Fig. 9(c) which is the plot of q_t vs $t^{1/2}$ shows the linearized regression fit. The plot showed that at each crude oil initial concentration, the line of regression slightly digressed from the origin without passing through it. The digression from the origin could be due to difference in the rate of mass transfer between the final and the initial bio-sorption stages. This digression from the origin indicates that there is the occurrence of low interfacial resistance (opposition) of the surrounding or encompassing film or some influence of boundary layer [54]. The relatively high R^2 values that ranged from 0.9000 to 0.9644 obtained for the different initial crude oil concentration as demonstrated by the model linear fit justifies why the mass transfer of oil into the plantain leaves bio-sorbent follows

intra-particle diffusion mechanism but being not the sole or the only controlling-rate (determining) step due to boundary layer influence. The determined values of the intra-particle diffusion rate constant, K_{w-m} and the intra-particle diffusivity, D_{id} are given in Table 11. It is observed that both the K_{w-m} and the D_{id} increased with rising initial concentration. The D_{id} values, 1.00–2.20 × 10^{-6} cm^2/s, which is found within the 10^{-6} to 10^{-8} cm^2/s range, suggest that the intra-partice diffusion is not the rate-determining step [76] of the crude oil bio-sorptive remediation by the plantain leaves. However, the values are also within the 10^{-5} - 10^{-12} cm^2/s range, the plantain leaves as bio-sorbent can be employed for chemisorption (i.e., chemical sorption) system [73,74].

3.9.4. Boyd et al. Particle and film diffusion model

Film diffusion and particle diffusion processes were the two forms of diffusion processes considered by Boyd et al. (1947) as provided in Equation 22a-c [74]:

$$F(t) = 1 - \frac{6}{\pi^2}\sum_{z=1}^{\infty}\frac{1}{z^2}\exp^{-z^2 B_t} \tag{22a}$$

$$B_t = \frac{-\pi^2 D_{eff}}{r^2} \tag{22b}$$

Where, $F(t)$, the equilibrium fractional attainment at time t; B_t, $F(t)$ mathematical function; D_{eff}, effective diffusion coefficient of sorbate (cm^2/s); r, radius of the bio-sorbent particle (m), and z is an integer. Values of $F(t)$ are obtained from Equation (22c):

$$F(t) = \frac{q_t}{q_e} \tag{22c}$$

Where q_t and q_e are experimental bio-sorption capacity at time t and experimental equilibrium bio-sorption capacity (g/g), respectively. Reichenberg [77], however modified Equation (22a) as given in Equation 23a - b by Yakub et al. [74]:

$$F(t)\text{values ranging from 0 to 0.85: } B_t = 2\pi - \frac{\pi^2 F}{3} - 2\pi\left(1 - \frac{\pi F}{3}\right)^{1/2} \tag{23a}$$

$$F(t)\text{values ranging from 0.86 to 1: } B_t = -\log_e\frac{\pi^2}{6}(1 - F) \tag{23b}$$

Hence, in ascertaining the actual determining-rate step, linearized plot of B_t against t (time) was done in differentiating between the film and particle diffusion-controlled bio-sorption. If the regression line went through the origin, then the rate of bio-sorption is particle diffusion governed. However, if the linear regression fit does not pass through the origin, the bio-sorption rate is film diffusion controlled or governed [74].

Fig. 9(d) depicts the Boyd et al. diffusion model plot of B_t against t at different initial concentration. As seen in Fig. 9(d), the linear regression fit line marginally deviated from the origin without passing through it; nevertheless, relatively displayed a high R^2 values that ranges from 0.9480 to 0.9985 (Table 11). However, these obtained R^2 values at the different crude oil initial concentration were relatively higher than the R^2 values, 0.9000 to 0.9644 obtained using Weber-Morris intra-particle diffusion model and therefore, indicates the relevance and dominance of film diffusion as a controlling or determining-rate factor in the plantain leaves-crude oil bio-sorption process. The determined or estimated values of the effective diffusion coefficients, D_{eff} are provided in Table 11. Table 11 shows that the film effective diffusion coefficients, D_{eff} generally increased as the crude oil initial concentration increased up till 7.8 g/L and above this concentration it started to decrease. The obtained D_{eff} values of 10^{-6} cm^2/s which is found within the 10^{-6} to 10^{-8} cm^2/s range imply that the rate-determining step of the crude oil bio-sorptive remediation by the plantain leaves is the film diffusion [76]. Also, these D_{eff} values of 10^{-6} are within the 10^{-5} to 10^{-12} cm^2/s range, which infers that plantain leaves as bio-sorbent can be utilized for chemisorption biosystem [73,74].

The relatively high R^2 values greater than 0.90 obtained for utilizing the bio-sorption and mass transfer models as presented in Table 9 indicates that the pseudo-first order and pseudo-second order-kinetic models as well as the Weber-Morris intra-particle diffusion and Boyd et al. diffusion models adequately adjusted well to the bio-sorptive remediation kinetics' data. Nevertheless, the crude oil-seawater system bio-sorptive remediation kinetics could suitably best be explained by the pseudo-second-order kinetic model as being the model that demonstrated the highest R^2 values of 0.9845–0.9957 at the various crude oil initial concentration. This implied that oil spill clean-up or removal from seawater utilizing plantain leaves as bio-sorbent agent follows the pseudo-second-order kinetics and that its bio-sorption mechanism is chemisorption. These findings and observations are in consonance with the findings and observations that were presented for the utilization of esterified coconut coir [70], bulrush [36], thermally and chemically modified coconut fibres [4] and *Annona senegalensis* [8] in oil spill clean-up from water.

4. Conclusions

The potential or feasibility of using plantain leaves as possible bio-sorbent for crude oil-seawater bio-sorptive remediation under different bio-sorptive remediation conditions or factors which includes, initial crude oil concentration, crude oil-seawater temperature, bio-sorbent dosage and bio-sorbent particle size was investigated and evaluated utilizing the $L_9 3^4$ type of TOAT. The TOAT was

also utilized to determine the optimal combination of the factors and their levels. The significant impact of the factors on the crude oil bio-sorption was determined using the S/N ratio analysis, ANOVA, and sigma values, respectively.

From this investigation, it was concluded that the effects of initial crude oil concentration, bio-sorbent dosage, and bio-sorbent on the crude oil-seawater bio-sorptive remediation were very significant while crude oil-seawater temperature has no significant influence on the oil bio-sorptive remediation. The bio-sorbent particle size was the major factor that affected the bio-sorption efficiency with its percentage contribution of 49.44 % followed by crude oil initial concentration (41.29 %) and bio-sorbent dosage having the least contribution (8.86 %). Predicted optimum factors' levels combination for achieving maximum or optimum bio-sorption efficiency and bio-sorption capacity can be obtained using the Taguchi S: NR analysis, the N-DOT and the proposed optimization method. The predicted optimum factors' levels combination obtained using these three different methods was $X_{11}X_{33}X_{41}$, at these combinations, the predicted optimum or maximum bio-sorption efficiency was 99.56 %, 99.57 % and 98.11 % using the Taguchi optimization technique, N-DOT and the proposed optimization method, respectively. At these predicted optimum factors' levels combination, the predicted optimum bio-sorption efficiency was experimentally validated or confirmed and was obtained to be 99.05 %. Similarly, the predicted optimum factors' levels combination obtained for bio-sorption capacity using these three different methods was $X_{13}X_{31}$, at these combinations, the predicted optimum or maximum bio-sorption efficiency was 12.98 g/g, 12.98 g/g and 11.04 g/g using the S:NR analysis of TOAT, N-DOT and the proposed optimization method, respectively. At these predicted optimum factors' levels combination, the actual experimentally validated optimum bio-sorption capacity was 12.82 g/g. The values of the percentage errors (−0.52 %, −0.52 % and 0.96 %) showed that there were no significant difference between the experimentally validated bio-sorption efficiency and the predicted bio-sorption efficiency using the S:NR analysis of TOAT, the N-DOT and the proposed optimization method. Also, the percentage errors between the experimentally validated bio-sorption capacity and the predicted bio-sorption capacity applying the S: NR analysis of TOAT, the N-DOT and the proposed optimization method were −1.25 %, −1.25 % and 14 %, and hence no significant variation between them. The regeneration/reusability study demonstrates that the biosorption efficiency for plantain leaves' bio-sorbent decreased from 99.05 % to 49.55 % at the end of five reusability cycles, while the biosorption capacity decreased from 12.82 g/g to 6.46 g/g.

Equilibrium bio-sorptive remediation data adequately adjusted very well to the Freundlich, Langmuir, and Temkin isotherm model equations. However, Freundlich isotherm model equation could best describe oil bio-sorption from seawater by plantain leaves-bio-sorbent having demonstrated very high R^2 value of 0.9991. That is, crude oil bio-sorption from water by plantain leaves as a bio-sorbent is a non-ideal heterogeneous bio-sorption process with the plantain leaves having a maximum bio-sorption capacity (K_f) of 14.00 g/g and bio-sorption intensity ($1/n$) of 0.516 at 25 °C.

The bio-sorptive remediation kinetics followed a pseudo-second-order kinetics and the plantain leaves-crude oil bio-sorption system being film diffusion-controlled while the bio-sorption occurs via dual mechanisms of physical-sorption (physisorption) and chemical sorption (chemisorption) with chemisorption showing more dominance. Therefore, plantain leaf has a strong potential for its application as a natural, viable, effective, and alternative bio-sorbent for the bio-sorptive remediation of seawater polluted with crude oil.

Funding

The authors did not receive support from any organization for the submitted work.

Data availability statement

Data associated with the study has not been deposited into any publicly available repository. Data associated with the study is included in the article.

CRediT authorship contribution statement

Blessing E. Eboibi: Conceptualization, Data curation, Formal analysis, Investigation, Methodology. **Michael C. Ogbue:** Conceptualization, Data curation, Formal analysis, Investigation, Methodology. **Esther C. Udochukwu:** Conceptualization, Data curation, Formal analysis, Investigation, Methodology. **Judith E. Umukoro:** Conceptualization, Data curation, Formal analysis, Investigation, Methodology. **Laura O. Okan:** Conceptualization, Data curation, Formal analysis, Investigation, Methodology. **Samuel E. Agarry:** Conceptualization, Formal analysis, Supervision, Visualization, Writing – original draft, Writing – review & editing. **Oluwafunmilayo A. Aworanti:** Conceptualization, Formal analysis, Supervision, Visualization, Writing – original draft, Writing – review & editing. **Oyetola Ogunkunle:** Data curation, Funding acquisition, Resources, Software, Writing – original draft, Writing – review & editing. **Opeyeolu T. Laseinde:** Data curation, Funding acquisition, Resources, Software, Writing – original draft, Writing – review & editing.

Declaration of competing interest

The authors declare that they have no known competing financial interests or personal relationships that could have appeared to influence the work reported in this paper.

References

[1] K. AlAmeri, A. Giwa, L. Yousef, A. Alraeesi, H. Taher, Sorption and removal of crude oil spills from seawater using peat-derived biochar: an optimization study, J. Environ. Manage. 250 (Nov. 2019), 109465, https://doi.org/10.1016/j.jenvman.2019.109465.

[2] N.A. Puasa, et al., Oil palm's empty fruit bunch as a sorbent material in filter system for oil-spill clean up, Plants 11 (1) (Jan. 2022) 127, https://doi.org/10.3390/plants11010127.

[3] O. Abdelwahab, S.M. Nasr, W.M. Thabet, Palm fibers and modified palm fibers adsorbents for different oils, Alexandria Eng. J. 56 (4) (2017) 749–755, https://doi.org/10.1016/j.aej.2016.11.020.

[4] S.E. Agarry, K.M. Oghenejoboh, E.O. Oghenejoboh, C.N. Owabor, O.O. Ogunleye, Adsorptive remediation of crude oil contaminated marine water using chemically and thermally modified coconut (Cocos nucifera) husks, J. Environ. Treat. Tech. 8 (2) (2020) 694–707.

[5] K.K. Dagde, Biosorption of crude oil spill using groundnut husks and plantain peels as adsorbents, Adv. Chem. Eng. Sci. 8 (3) (2018) 161–175, https://doi.org/10.4236/aces.2018.83011.

[6] A. Tuan Hoang, V. Viet Pham, D. Nam Nguyen, A Report of Oil Spill Recovery Technologies, 2018 [Online]. Available: http://www.ripublication.com.

[7] M. Hassanshahian, G. Emtiazi, G. Caruso, S. Cappello, Bioremediation (bioaugmentation/biostimulation) trials of oil polluted seawater: a mesocosm simulation study, Mar. Environ. Res. 95 (Apr. 2014) 28–38, https://doi.org/10.1016/j.marenvres.2013.12.010.

[8] B.J. Dimas, S.A. Osemeahon, Utilization of Annona senegalensis as a sorbent for THE removal of crude oil from aqueous Media, J. Energy Res. Rev. 7 (4) (Jun. 2021) 68–82, https://doi.org/10.9734/jenrr/2021/v7i430199.

[9] B.Y. Eweida, A.M. Omer, T.M. Tamer, H.A.-E.M. Soliman, A.A. Zaatot, M.S. Mohy-Eldin, Kinetics, isotherms and thermodynamics of oil spills removal by novel amphiphilic Chitosan-g-Octanal Schiff base polymer developed by click grafting technique, Polym. Bull. 80 (5) (2023) 4813–4840, https://doi.org/10.1007/s00289-022-04260-9.

[10] Y. Yu, N. Chen, W. Hu, C. Feng, Application of Taguchi experimental design methodology in optimization for adsorption of phosphorus onto Al/Ca-impregnated granular clay material, Desalin. Water Treat. 56 (11) (Oct. 2014) 1–11, https://doi.org/10.1080/19443994.2014.963687.

[11] M. Khosravi, S. Azizian, Synthesis of a novel highly oleophilic and highly hydrophobic sponge for rapid oil spill cleanup, ACS Appl. Mater. Interfaces 7 (45) (Nov. 2015) 25326–25333, https://doi.org/10.1021/acsami.5b07504.

[12] J. Ge, et al., Joule-heated graphene-wrapped sponge enables fast clean-up of viscous crude-oil spill, Nat. Nanotechnol. 12 (5) (2017) 434–440, https://doi.org/10.1038/nnano.2017.33.

[13] O.A. Galblaub, I.G. Shaykhiev, S.V. Stepanova, G.R. Timirbaeva, Oil spill cleanup of water surface by plant-based sorbents: Russian practices, Process Saf. Environ. Prot. 101 (May 2016) 88–92, https://doi.org/10.1016/j.psep.2015.11.002.

[14] B.M. Omar, S.A. Abdelgalil, H. Fakhry, et al., Wheat husk-based sorbent as an economical solution for removal of oil spills from sea water, Sci. Report. 13 (2023) 2575, https://doi.org/10.1038/s41598-023-29035-8.

[15] R.N. Malhas, K.W. Amadi, Oil removal from polluted seawater using carbon avocado peel as bio-Absorbent, European J. Eng. Technol. Res. 8 (2) (2023) 26–32, https://doi.org/10.24018/ejeng.2023.8.2.3004.

[16] J.C. Onwuka, E.B. Agbaji, V.O. Ajibola, F.G. Okibe, Treatment of crude oil-contaminated water with chemically modified natural fiber, Appl. Water Sci. 8 (3) (2018) 86, https://doi.org/10.1007/s13201-018-0727-5. Jun.

[17] H.-J. Choi, Agricultural bio-waste for adsorptive removal of crude oil in aqueous solution, J. Mater. Cycles Waste Manag. 21 (2) (2019) 356–364, https://doi.org/10.1007/s10163-018-0797-3. Mar.

[18] F.T. Ademiluyi, H. Omorogbe, K.K. Dune, S.O.N. Dimkpa, Adsorption of crude oil in aqueous Medium using dried plantain (*Musa paradisiaca*) leaves and peels, J. Newviews Eng. Technol. 2 (3) (2020) 54–65 [Online]. Available: http://www.rsujnet.org/index.php/publications/2020-edition.

[19] C.O. Asadu, E.C. Anthony, O.C. Elijah, I.S. Ike, O.E. Onoghwarite, U.E. Okwudili, Development of an adsorbent for the remediation of crude oil polluted water using stearic acid grafted coconut husk (*Cocos nucifera*) composite, Appl. Surf. Sci. Adv. 6 (Dec. 2021), 100179, https://doi.org/10.1016/j.apsadv.2021.100179.

[20] C.O. Asadu, et al., Treatment of crude oil polluted water using stearic acid grafted mango seed shell (*Mangifera indica*) composite, Curr. Res. Green Sustain. Chem. 4 (2021), 100169, https://doi.org/10.1016/j.crgsc.2021.100169.

[21] N.O. Ogbodo, et al., Preparation and Characterization of activated carbon from agricultural waste (Musa-paradisiaca peels) for the remediation of crude oil contaminated water, J. Hazard. Mater. Adv. 2 (2021), 100010, https://doi.org/10.1016/j.hazadv.2021.100010. Oct.

[22] S.C. Cheu, H. Kong, S.T. Song, N. Saman, K. Johari, H. Mat, High removal performance of dissolved oil from aqueous solution by sorption using fatty acid esterified pineapple leaves as novel sorbents, RSC Adv. 6 (17) (2016) 13710–13722, https://doi.org/10.1039/C5RA22929D.

[23] W.S. Jaber, A.I. Alwared, Removal of oil emulsion from aqueous solution by using Ricinus communis leaves as adsorbent, SN Appl. Sci. 1 (8) (2019) 944, https://doi.org/10.1007/s42452-019-0970-x. Aug.

[24] F. Hassan, A.M. Ashraf Sabri, A. Sarosh, N. Ullah, Use of neem leaves for oil removal from waste water Pak, J. Engg. Appl. Sci. 23 (July) (2018) 86–92.

[25] J. Tari Honda, M. Yelwa, J, A.N. Ulteino, S. Abudllahi, A. S U, H.G. Anchau, K. Michael Kalu, Optimization of biosorption conditions for crude oil spills using acetylated and Unacetylated biosorbents derived from Cissus populnea leaves stem and roots, International Journal of Science and Environment (IJSE) 3 (2) (2023) 51–65, https://doi.org/10.51601/ijse.v3i2.67.

[26] M.A. Mahmoud, A.M. Tayeb, A.M. Daher, O.Y. Bakather, M. Hassan, et al., Adsorption study of oil spill cleanup from sea water using natural sorbent, Chemical Data Collections 41 (2022), 100896, https://doi.org/10.1016/j.cdc.2022.100896.

[27] S.Y. Ang, N.F.N. Nasaruddin, H.N. Abdul Halim, S.K. Mahmad Rozi, Z. Mokhtar, L.S. Tan, N.W. Che Jusoh, Potential of fatty acid-modified spent tea leaves as adsorbent for oil adsorption, Progress in Energy and Environment 17 (2022) 32–41, https://doi.org/10.37934/progee.17.1.3241.

[28] S.R. Korake, P.D. Jadhao, Investigation of Taguchi optimization, equilibrium isotherms, and kinetic modeling for cadmium adsorption onto deposited silt, Heliyon 7 (1) (Jan. 2021), e05755, https://doi.org/10.1016/j.heliyon.2020.e05755.

[29] J.S. Lupoi, et al., Localization of polyhydroxybutyrate in sugarcane using Fourier-transform infrared microspectroscopy and multivariate imaging, Biotechnol. Biofuels 8 (1) (2015) 98, https://doi.org/10.1186/s13068-015-0279-y. Dec.

[30] R. Davis, P. John, Application of taguchi-based design of experiments for Industrial chemical processes, in: Statistical Approaches with Emphasis on Design of Experiments Applied to Chemical Processes, InTech, 2018, pp. 137–155.

[31] G. Mosoarca, C. Vancea, S. Popa, S. Boran, Optimization of crystal violet adsorption on common lilac tree leaf powder as natural adsorbent material, Glob. Nest J. 24 (1) (2022), https://doi.org/10.30955/gnj.003951.

[32] G. Nagpal, A. Bhattacharya, N.B. Singh, Cu(II) ion removal from aqueous solution using different adsorbents, Desalin. Water Treat. 57 (21) (May 2016) 9789–9798, https://doi.org/10.1080/19443994.2015.1032364.

[33] P.T. Dhorabe, D.H. Lataye, A.R. Tenpe, R.S. Ingole, Adsorption of p-nitrophenol onto acacia glauca saw dust and waste orange peels activated carbon: application of Taguchi's design of experiment, SN Appl. Sci. 1 (3) (2019), https://doi.org/10.1007/s42452-019-0264-3.

[34] H. Aguedal, A. Iddou, J. Locs, Optimization of the adsorption process of Bezaktiv Turquoise blue «VG» textile dye onto Diatomite using the taguchi method, Key Eng. Mater. 762 (Feb. 2018) 81–86, https://doi.org/10.4028/www.scientific.net/KEM.762.81.

[35] S.E. Agarry, Statistical optimization and kinetic studies of enhanced bioremediation of crude oil - contaminated marine water using combined adsorption-biostimulation strategy, J. Appl. Sci. Environ. Manag. 21 (1) (2017) 59, https://doi.org/10.4314/jasem.v21i1.7.

[36] M.A. Oraibi, Study the individual performance of bulrush as a natural sorbent to remove oil layer from simulated sea water for isothermal batch processes, Int. J. Eng. Res. Technol. 12 (12) (2019) 2289–2293.

[37] A.M. Gorshkov, I.S. Khomyakov, A.S. Mazurova, Some aspects to develop method for determining the open porosity of ultralow-permeability rocks on crushed core, IOP Conf. Series: Earth and Environmental Science 459 (2020), 022068, https://doi.org/10.1088/1755-1315/459/2/022068.

[38] H. Serencam, A. Özdemir, Ç. Teke, M. Uçurum, Modeling design parameters with taguchi experimental method for obtaining operating conditions for cu(Ii) removal through adsorption process, Desalin. Water Treat. 167 (2019) 269–276, https://doi.org/10.5004/dwt.2019.24617.

[39] A. Fathollahi, S.J. Coupe, A.H. El-Sheikh, E.O. Nnadi, Cu(II) biosorption by living biofilms: isothermal, chemical, physical and biological evaluation, J. Environ. Manage. 282 (Mar. 2021), 111950, https://doi.org/10.1016/j.jenvman.2021.111950.

[40] B.A. Olufemi, F. Otolorin, Comparative adsorption of crude oil using mango (Mangnifera indica) shell and mango shell activated carbon, Environ. Eng. Res. 22 (4) (2017) 384–392, https://doi.org/10.4491/eer.2017.011.

[41] S.M. Sidik, A.A. Jalil, S. Triwahyono, S.H. Adam, M.A.H. Satar, B.H. Hameed, Modified oil palm leaves adsorbent with enhanced hydrophobicity for crude oil removal, Chem. Eng. J. 203 (Sep. 2012) 9–18, https://doi.org/10.1016/j.cej.2012.06.132.

[42] C.O. Asadu, et al., Equilibrium isotherm modelling and optimization of oil layer removal from surface water by organic acid grafted plantain pseudo stem fiber, Case Stud. Chem. Environ. Eng. 5 (May 2022), 100194, https://doi.org/10.1016/j.cscee.2022.100194.

[43] K. Sathasivam, M.R.H. Mas Haris, Adsorption kinetics and capacity of fatty acid-modified banana Trunk fibers for oil in water, Water, Air, Soil Pollut 213 (1–4) (Nov. 2010) 413–423, https://doi.org/10.1007/s11270-010-0395-z.

[44] N.T. Ha, L. Van Cat, P.V. Anh, T. Thi, T. Lien, Research on oil adsorption capacity of Carbonized material derived from agricultural by-product (Corn Cob , Corn Stalk , rice husk) using in oily Wastewater Treatment, Nat. Sci. Technol. 32 (3) (2016) 105–111.

[45] S.S. Saravanakumar, A. Kumaravel, T. Nagarajan, I.G. Moorthy, Effect of chemical Treatments on Physicochemical properties of Prosopis juliflora fibers, Int. J. Polym. Anal. Charact. 19 (5) (Jan. 2014) 383–390, https://doi.org/10.1080/1023666X.2014.903585.

[46] S. Yildiz, Kinetic and isotherm analysis of Cu(II) adsorption onto Almond shell (Prunus Dulcis), Ecol. Chem. Eng. S 24 (1) (Mar. 2017) 87–106, https://doi.org/10.1515/eces-2017-0007.

[47] I. Jansson, F.J. García-García, B. Sánchez, S. Suárez, Key factors to develop hybrid photoactive materials based on mesoporous carbon/TiO2 for removal of volatile organic compounds in air streams, Appl. Catal. Gen. 623 (2021), 118281.

[48] B.D. Zdravkov, J.J. Čermák, M. Šefara, J. Janků, Pore classification in the characterization of porous materials: a perspective, Central Eur. J. Chem. 5 (2) (2007) 385–395.

[49] M.A. Martín-González, P. Susial, J. Pérez-Peña, J.M. Doña-Rodríguez, Preparation of activated carbons from banana leaves by chemical activation with phosphoric acid. Adsorption of methylene blue, Rev. Mex. Ing. Quim. 12 (3) (2013) 595–608.

[50] A. Li, W. Huang, N. Qiu, F. Mou, F. Wang, Porous carbon prepared from lotus leaves as potential adsorbent for efficient removal of rhodamine B, Mater. Res. Express 7 (5) (2020), 055505, https://doi.org/10.1088/2053-1591/ab8dcf.

[51] A. Abdulkareem, et al., The separation of emulsified water/oil mixtures through adsorption on plasma-treated polyethylene powder, Materials 14 (5) (2021) 1, https://doi.org/10.3390/ma14051086.

[52] B. E. Eboibi, E. C. Udochukwu, M. C. Ogbue, J. O. Umukoro, L. O. Okan & S. E. Agarry Bio-sequestration of crude oil from seawater by bio-adsorption onto oil palm (*Elaeis guineensis*) fruit mesocarp fibre: taguchi process optimization, batch isotherm and kinetic modelling studies. J. Dispersion Sci. Technol., 1-19. DOI: 10.1080/01932691.2023.2228883.

[53] F.A. Dawodu, U.N. Obioha, K.G. Akpomie, Removal OF crude oil from aqueous solution BY zinc chloride modified DIOSCOREA ROTUNDATA peel carbon: equilibrium, kinetic and INTRAPARTICLE diffusivity, Pet. Coal 60 (5) (2018) 985–994.

[54] S.E. Agarry, Anthracene Bioadsorption from simulated Wastewater by chemically-treated Unripe plantain peel Bioadsorbent: batch kinetics and isothermal modeling studies, Polycycl. Aromat. Compd. 39 (1) (2019) 23–43, https://doi.org/10.1080/10406638.2016.1255650.

[55] S. Agarry, Batch equilibrium and kinetic studies of simultaneous adsorption and Biodegradation of phenol by pineapple peels Immobilized Pseudomonas aeruginosa NCIB 950, Br. Biotechnol. J. 2 (1) (2012) 26–48, https://doi.org/10.9734/bbj/2012/902.

[56] S.E. Agarry, O.O. Ogunleye, Bioadsorption of 2, 6-Dichlorophenol from aqueous solution onto plantain and pineapple peels mixture used as adsorbent, Chem. Mater. Res. 7 (3) (2015) 1–15.

[57] M.K.P. Koh, J. Sun, S.Q. Liu, Optimization of L-methionine Bioconversion to Aroma-active Methionol by Kluyveromyces lactis using the taguchi method, J. Food Res. 2 (4) (2013) 90, https://doi.org/10.5539/jfr.v2n4p90. Jul.

[58] K. Yadolahi, A. Ghadi, S.A. Alavi, Optimization of copper adsorption process from aqueous solution by descurainia sophia plant stem using taguchi method, J. Water Environ. Nanotechnol. 5 (1) (2020), https://doi.org/10.22090/jwent.2020.01.006.

[59] J.A. Al-Najar, S.T. Al-Humairi, T. Lutfee, D. Balakrishnan, I. Veza, M.E.M. Soudagar, I.M.R. Fattah, Cost-effective natural adsorbents for remediation of oil-contaminated water, Water 15 (2023) 1186, https://doi.org/10.3390/w15061186.

[60] O. Abdelwahab, Assessment of raw luffa as a natural hollow oleophilic fibrous sorbent for oil spill cleanup, Alex. Eng. J. 53 (2014) 213–218.

[61] I.A. El Gheriany, F. Ahmad El Saqa, A. Abd El Razek Amer, M. Hussein, Oil spill sorption capacity of raw and thermally modified orange peel waste, Alex. Eng. J. 59 (2020) 925–932.

[62] M. Husseien, A.A. Amer, A. El-Maghraby, N.A. Taha, Availability of barley straw application on oil spill clean-up, Int. J. Environ. Sci. Technol. 6 (2009) 123–130.

[63] G. Alaa El-Din, A.A. Amer, G. Malsh, M. Hussein, Study on the use of banana peels for oil spill removal, Alex. Eng. J. 57 (2018) 2061–2068.

[64] R. Behnood, B. Anvaripour, N. Jaafarzadeh, M. Farasati, Oil spill sorption using raw and acetylated sugarcane bagasse, J. Cent. South Univ. 23 (2016) 1618–1625.

[65] K.K. Kudaybergenov, E.K. Ongarbayev, Z.A. Mansurov, Petroleum sorption by thermally treated rice husks derived from agricultural byproducts, Eurasian Chem. J. 15 (2012) 57.

[66] A.D.F. Alsulaili, M. Asmaa, Oil removal from produced water by agriculture waste adsorbents, Int. J. Environ. Waste Manag. 25 (2020) 12–31.

[67] D.A. Benjamin, E. Zahir, M.A. Asghar, On the practicability of a new bio sorbent: Lasani sawdust and coconut coir for cleanup of oil spilled on water, Pet. Sci. Technol. 37 (2019) 1143–1154.

[68] J. Zou, X. Liu, W. Chai, X. Zhang, Li, B, Y. Wang, Y. Ma, Sorption of oil from simulated seawater by fatty acid-modified pomelo peel, Desalination Water Treat. 56 (4) (2014) 939–946.

[69] M. Mojžiš, T. Bubeníková, M. Zachar, D. Kăcíková, J. Štefková, Comparison of natural and synthetic sorbents' efficiency at oil spill removal, Bioresources 14 (2019) 8738–8752.

[70] N.A. Yusof, H. Mukhair, E.A. Malek, F. Mohammad, Esterified coconut coir by fatty acid chloride as biosorbent in oil spill removal, Bioresources 10 (4) (Oct. 2015) 8025–8038, https://doi.org/10.15376/biores.10.4.8025-8038.

[71] K. Okiel, M. El-Sayed, M.Y. El-Kady, Treatment of oil–water emulsions by adsorption onto activated carbon, bentonite and deposited carbon, Egypt. J. Pet. 20 (2) (2011) 9–15, https://doi.org/10.1016/j.ejpe.2011.06.002.

[72] G. Sánchez-Galván, F.J. Mercado, E.J. Olguín, Leaves and roots of Pistia stratiotes as sorbent materials for the removal of crude oil from saline solutions, Water, Air, Soil Pollut 224 (2) (2013) 1421, https://doi.org/10.1007/s11270-012-1421-0. Feb.

[73] C.R. Girish, V.R. Murty, Mass transfer studies on adsorption of phenol from Wastewater using Lantana camara , forest waste, Int. J. Chem. Eng. 2016 (2016) 1–11, https://doi.org/10.1155/2016/5809505.

[74] E. Yakub, S.E. Agarry, F. Omoruwou, C.N. Owabor, Comparative study of the batch adsorption kinetics and mass transfer in phenol-sand and phenol-clay adsorption systems, Part. Sci. Technol. 38 (7) (Oct. 2020) 801–811, https://doi.org/10.1080/02726351.2019.1616862.

[75] J.O. Vinhal, K.K. Nege, M.R. Lage, J.W. de M. Carneiro, C.F. Lima, R.J. Cassella, Adsorption of the herbicides diquat and difenzoquat on polyurethane foam: kinetic, equilibrium and computational studies, Ecotoxicol. Environ. Saf. 145 (Nov. 2017) 597–604, https://doi.org/10.1016/j.ecoenv.2017.08.005.

[76] P. Shanthi, G. Tamilarasan, K. Anitha, K. Sathasivam, Film and pore diffusion modeling for adsorption of reactive red-4 onto Sterculia quadrifida seed shell waste as activated carbon, Rasayan Jourbal Chem 7 (3) (Jan. 2014) 229–240.

[77] D. Reichenberg, Properties of ion-Exchange Resins in relation to their Structure. III. Kinetics of Exchange, J. Am. Chem. Soc. 75 (3) (Feb. 1953) 589–597, https://doi.org/10.1021/ja01099a022.